



- 1 A comprehensive review of tropospheric background
- 2 ozone: Definitions, estimation methods, and meta-analysis
- 3 of its spatiotemporal distribution in China
- 4 Chujun Chen¹, Weihua Chen^{1*}, Linhao Guo¹, Yongkang Wu¹, Xianzhong Duan¹,
- 5 Xuemei Wang¹, Min Shao¹

9

10

11

12

13

14

15

16

17

18

19

20

21

22

23

24

25

26

- 6 ¹College of Environmental and Climate, Jinan University, Guangzhou, 510632, P. R. China
- 7 *Correspondence: Weihua Chen (chenwh26@jnu.edu.cn)

Abstract. Background ozone (O₃) refers to O₃ concentrations that remain unaffected by direct local anthropogenic emissions, critical for comprehending tropospheric O₃ pollution, as it defines the baseline levels without local anthropogenic emissions. Accurately estimating background O3 is essential for determining the maximum achievable reductions in O₃ through anthropogenic precursor emissions control and for developing effective air quality management strategies. This review synthesizes the definition and estimation methods for background O3, including in situ measurement, statistical analysis, numerical modeling, and integrated method. A meta-analysis of the spatiotemporal distribution of background O3 across China from 1994 to 2020 reveals substantial spatial variability, with the highest concentrations in the Northwest region (48 ppb) and the lowest in the Northeast and Central regions (~33 ppb). The national average background O₃ concentration is approximately 40 ppb, contributing 77 % to the tropospheric maximum daily 8-hour average ozone. Estimation methods show notable discrepancies: in situ measurement and statistical analysis methods yield higher estimates, while integrated method provide lower yet more consistent values. On a global scale, background O3 concentrations in China are ranked medium-to-high and exhibit an increasing trend. This review, from a global perspective, highlights the need for integrated estimation methods to improve accuracy, underscores the importance of international collaboration in addressing long-range pollutant transport, and calls for further research on the interactions between background O₃ and climate change. By advancing the understanding of background O3 dynamics, this study provides critical insights for atmospheric chemistry research and air pollution control efforts in China and beyond.





1 Introduction

27

28

29

30

31

32

33

34

35

36

37

38

39

40

41

42

43

44

45

46

47

48

49

50

51

52

53

subsequent "Three-Year Action Plan for Winning the Blue Sky War", China has made significant progress in air quality management, particularly in reducing fine particulate matter (PM2.5) concentrations. These policies have been effective in curbing PM2.5 levels, with nationwide PM2.5 concentrations declining by approximately 50 % from 2013 to 2020 (Geng et al., 2024). However, despite these successes in controlling PM2.5, the annual average concentration of ozone (O3) in major urban clusters has exhibited a persistent upward trend. From 2015 to 2022, the frequency of O₃ pollution days has steadily increased, with urban areas such as Beijing, Shanghai, and Guangzhou experiencing a marked rise in O₃ concentrations (Li et al., 2019; Wang et al., 2023). Notably, large-scale, prolonged O₃ pollution episodes have also become more frequent, with the number of days exceeding the national O₃ standard more than doubling in some regions over the past decade (Ozone Pollution Control Committee of Chinese Society of Environmental Sciences, 2024). Therefore, the "Opinions on Deepening the Fight Against Pollution", issued by the Central Committee of the Communist Party of China and the State Council, acknowledged these challenges and explicitly mandated that the coordinated control of both PM_{2.5} and O₃ should be incorporated into the "14th Five-Year Plan" (2021-2025), signaling a new phase in addressing multi-pollutant control. O₃ is a secondary pollutant formed through complex photochemical reactions involving volatile organic compounds (VOCs) and nitrogen oxides (NO_x). Tropospheric O₃ refers to O₃ in the lower part of the atmosphere and consists of two primary components: O3 produced from anthropogenic precursor emissions and background O3, both of which directly impacts human health, ecological ecosystems, and agricultural productivity (McDonald-Buller et al., 2011; Wang et al., 2009b). Background O₃ refers to the portion of O₃ concentrations that remain unaffected by direct local anthropogenic emissions. Its sources are diverse, including natural emissions from vegetation, soil, lightning, and wildfires, as well as O₃ produced from methane (CH₄) oxidation, stratosphere-troposphere exchange (STE), and the longrange transport of pollutants, as shown in Fig. 1 (Dolwick et al., 2015; Thompson, 2019). It is important to note that in the pre-industrial era (~1750), CH₄ emissions were overwhelmingly dominated by natural

Since the implementation of the "Air Pollution Prevention and Control Action Plan" in 2013 and the

55

56

57

58

59

60

61

62

63

64

65

66

67

68

69

70

71

72

73

74

75

76

77

78

79

80





sources (e.g., wetlands, inland freshwaters, and geological), accounting for approximately 95% of global emissions (Lassey et al., 2000; Prather et al., 2012; Valdes et al., 2005), which contributed to relatively stable atmospheric CH₄ concentrations (Ehhalt et al., 2001; Wuebbles and Hayhoe, 2002). Owing to its long atmospheric lifetime (8-9 years) and well-mixed global distribution, CH4 played a crucial role in sustaining background O₃ levels on a global scale (Fiore et al., 2002; Vingarzan, 2004; West and Fiore, 2005; Thompson, 2019). Accordingly, CH₄ oxidation has traditionally been regarded as a contributor to background O₃ (Skipper et al., 2021; Sun et al., 2024; Thompson, 2019; Vingarzan, 2004; Wu et al., 2008). However, with the intensification of anthropogenic activities, the proportion of CH4 emissions attributable to human sources (e.g., agriculture, fossil fuels, landfills and waste) has risen markedly from 31% in 1850 to 61 % by 2012 (Fiore et al., 2002; Jackson et al., 2024; Kirschke et al., 2013; Lelieveld et al., 1998; Saunois et al., 2016). In light of this shift, the contribution of anthropogenically derived CH₄ to O3 formation can no longer be classified as part of the background component. To improve the accuracy of background O3 assessments, it is therefore essential that future studies explicitly differentiate and exclude the influence of anthropogenic CH₄ emissions. Background O₃, primarily influenced by natural sources and large-scale environmental factors (e.g., long-range transport of pollutants, and regional meteorological conditions), typically contributes 60-80 % of total tropospheric O₃ at both global and regional scales (Akimoto et al., 2015; Chen et al., 2022; Dolwick et al., 2015; Lee and Park, 2022; Lefohn et al., 2014; Zhang et al., 2011). Unlike PM2.5, which can be more directly controlled through emission reductions, the management of O₃ is more complex and has become a significant challenge in global air quality governance (Chen et al., 2022). Research has shown that reductions in anthropogenic precursor emissions of O₃ have led to declines in pollution episodes in regions such as Europe, the United States, and Japan. However, background O₃ concentrations continue to rise, complicating efforts to reduce overall ground-level O₃ pollution (Akimoto et al., 2015; Cooper et al., 2012; Wilson et al., 2012; Yan et al., 2021). For example, studies from the United States show that while emissions reductions have resulted in fewer O₃ exceedance days, the relative contribution of background O₃ to total ground-level O₃ has risen by approximately 6 % over the past two decades (Jaffe et al., 2018). In recent years, environmental changes such as global climate

82

83

84

85

86

87

88

89

90

91

92

93

94

95

96

97

98

99

100

101

102

103

104

105

106

107





change, increased CH4 emissions, and transboundary pollution have led to a steady increase in background O₃ levels (Chen et al., 2022; Vingarzan, 2004). This rise is particularly evident in regions like East Asia, where transboundary pollution from neighboring countries exacerbates the problem (Vingarzan, 2004). Furthermore, as emissions of anthropogenic precursors continue to be controlled, it is projected that the relative contribution of background O₃ to overall O₃ pollution will become increasingly significant (Jaffe et al., 2018; Lam and Cheung, 2022; Skipper et al., 2021). This shift will require a rethinking of air quality management strategies, with greater emphasis on mitigating the factors influencing background O3 levels, such as reducing global CH4 emissions and addressing transboundary pollution. Unlike O₃ formed from anthropogenic precursors, background O₃ cannot be mitigated through local emission reductions. Instead, it represents the "baseline" level for regional O₃ pollution, determining the maximum achievable reduction in ground-level O3 through local anthropogenic emission controls (Fiore et al., 2014; Wang et al., 2009a; Zhang et al., 2011). The increasing levels of background O₃ are complicating air quality management because they limit the effectiveness of local emission reductions (Thompson, 2019; Vingarzan, 2004). In regions such as the United States and Europe, elevated levels of background O₃ undermine the effectiveness of ongoing efforts to meet current O₃ standards and present a major obstacle to meeting more stringent future standards (Thompson, 2019; Vingarzan, 2004). The persistence of high background O₃ levels has become a critical area of scientific and policy research worldwide. For example, the National Aeronautics and Space Administration (NASA) has highlighted background O₃ as a priority issue in efforts to reduce O₃ pollution in the United States (Huang et al., 2015). Similarly, the "China Blue Book on Prevention and Control of Atmospheric Ozone Pollution (2020) " recognizes urban O₃ pollution and regional background O₃ concentrations as significant challenges for future O₃ management and emphasizes the need for advanced research to better understand regional variations in background O3 concentrations and their impact on local air quality (Ozone Pollution Control Committee of Chinese Society of Environmental Sciences, 2022). The complexity and global implications of background O₃ make it an essential focus of research in

atmospheric chemistry, climate change, and air quality management. Its contribution to total tropospheric

https://doi.org/10.5194/egusphere-2025-687 Preprint. Discussion started: 28 March 2025 © Author(s) 2025. CC BY 4.0 License.

108

109

110

111

112

113

114

115

116

117

118

119

120

121

122

123





O3 concentrations is both substantial and difficult to control, as it is influenced by a range of natural and anthropogenic factors beyond the immediate control of local emission regulations. Despite its growing importance, key gaps remain in understanding the sources, variability, and impacts of background O3. This study aims to provide a comprehensive review of the definitions and estimation methods for background O₃, offering a foundation for advancing scientific understanding in this area. By utilizing publicly available datasets, we systematically examine the spatial and temporal variations of background O₃ across China, uncovering regional heterogeneities, discrepancies between different estimation methods, and key influencing factors. Additionally, we conduct a comparative analysis of China's background O3 levels with those in other global regions, providing a broader context for understanding the dynamics of background O3 in the face of global environmental change. This comparative analysis not only reveals the distinct challenges China faces in managing O₃ pollution but also provides broader insights into regional difference in background O₃, reinforcing the importance of the global outlook in addressing this issue. Finally, we propose potential directions for future research on background O₃, emphasizing the importance of filling existing knowledge gaps in this field. As background O₃ continues to influence the effectiveness of O₃ mitigation efforts, this research is pivotal for shaping future air quality management strategies and ensuring the protection of public health and ecosystems.





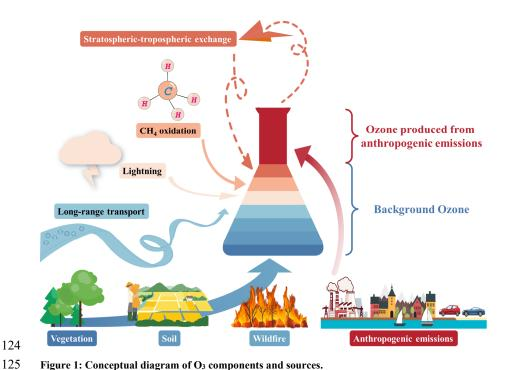


Figure 1: Conceptual diagram of O₃ components and sources.

2 Materials and methods

126

127

128

129

130

131

132

133

134

135

136

137

2.1 Data source and study area

To provide a comprehensive synthesis of advancements in the study of background O₃, a systematic literature search was conducted across major academic databases, including the Web of Science, Google Scholar, Science Direct (Elsevier), Scopus, Springer, Wiley, and China National Knowledge Infrastructure (CNKI). The search was centered on the following key thematic terms: background/baseline/natural, ozone/O3, regional background ozone/O3, and policy relevant background ozone/O₃, ensuring the inclusion of a wide range of relevant studies. This study identified 171 pertinent documents, comprising 134 peer-reviewed English-language papers, 25 peer-reviewed Chinese-language papers, 4 English-language reports, 4 English-language books, 2 Chinese-language books, and 2 Chinese-language master's theses. These documents form the core foundation of this review, which traces the evolution of the definition and estimation method for background O3 over a span of seven

139

140

141

142

143

144

145

146

147

148

149

150

151

152

153

154

155

156

157

158

159

160

161

162





decades (1952-2024), providing a comprehensive historical perspective on the development of the field. In addition to reviewing the definition and estimation method for background O3, we also analyzed the spatial and temporal characteristics of regional background O3 concentrations in China during the period 1994-2020. This analysis was based on 44 peer-reviewed papers, including 28 papers in English and 16 papers in Chinese, which collectively provided over 700 data points on background O₃ concentration from various regions and time periods within China. The dataset includes diverse temporal resolutions, such as annual data (31 %, 237 data points), seasonal data (26 %, 195 data points), and monthly data (43 %, 326 data points). To offer a deeper understanding of the seasonal distribution of data, the seasonal and monthly data were further categorized as follows: spring (24 %, 127 data points), summer (28 %, 145 data points), autumn (24 %, 125 data points), and winter (24 %, 124 data points). The seasonal divisions were based on standard meteorological periods: spring (March-May), summer (June-August), autumn (September-November), and winter (December-February). Detailed information on the collected data, including a breakdown of regional and temporal distributions, is provided in Table S1. To assess the regional differences in background O3 concentrations across China, the country was categorized into seven geo-administrative regions based on a combination of social, natural, economic, and human environmental factors (He et al., 2023). These regions include Northeast China (NEC), North China (NC), East China (EC), Central China (CC), Northwest China (NWC), Southwest China (SWC), and South China (SC), as shown in Fig. 4. A detailed description of these regional divisions is provided in Table S2.

2.2 Data process

The background O_3 concentrations presented in this study are expressed as molar mixing ratios in parts per billion (ppb). In some literature, the background O_3 concentrations are reported in micrograms per cubic meter ($\mu g \, m^{-3}$). To ensure consistency with international standard units and facilitate comparisons with global datasets, unit conversion was performed using the following Eq. (1):

163
$$ppb = \left(\frac{22.4 \,\mathrm{L} \,\mathrm{mol}^{-1}}{48 \,\mathrm{g} \,\mathrm{mol}^{-1}}\right) \times (\mu \mathrm{g} \,\mathrm{m}^{-3}),$$
 (1)





165 and pressure (101.325 kPa), while 48 g mol⁻¹ is the molar mass of O₃. 166 2.3 Trend analysis 167 This study employed linear regression analysis to examine the annual trend in background O₃ 168 concentration and assess the statistical significance of these trends over time. Specifically, linear 169 regression was applied to a scatter plot of background O3 concentrations across different years, using the 170 least squares to determine the relationship between background O₃ concentration and time. 171 To evaluate the model's performance, the coefficient of determination (R²) was calculated. R² 172 represents the proportion of variance in background O₃ concentration explained by the linear model, 173 indicating how well the model fits the observed data. Higher R2 values suggest a strong fit, while lower 174 values indicate a weaker fit. The P-value was also calculated to test the statistical significance of the 175 linear relationship between background O3 concentration and time. A smaller P-value (typically less than 176 0.05) indicates a statistically significant linear relationship, suggesting that the observed trend is unlikely 177 to have occurred by chance. In contrast, larger P-values imply that the trend may not be statistically 178 significant and could result from random variation. 179 It is important to note that, for the analysis of interannual variations in background O₃ concentration, 180 only annual data from our compiled data set were used. Data points from individual studies that 181 significantly deviated from the overall trend were excluded to ensure the robustness of the analysis. 182 However, consecutive data points with large deviations were retained for consistency. Furthermore, when 183 background O₃ concentrations were derived using different methods in the same geographical region 184 within the same study, the results were averaged to provide a more representative value. 185 3 Background ozone: conceptual evolution and key definitions 186 Background O₃ generally refers to the portion of O₃ concentrations that are not influenced by direct local 187 anthropogenic emissions, though its definition varies across studies globally. In contemporary 188 atmospheric research, background O₃ is commonly categorized into two distinct types: natural 189 background ozone (NBO) and regional background ozone (RBO). These two categories are crucial for

Where 22.4 L mol⁻¹ represents the molar volume of an ideal gas at standard temperature (0 °C)





190 understanding the sources and variations of background O₃ on both local and global scales. Figure 2 191 presents the evolution of background O3 definitions. 192 Natural background ozone (NBO) refers to O3 that forms exclusively through natural processes, 193 independent of anthropogenic emissions (McDonald-Buller et al., 2011; Vingarzan, 2004; Wu et al., 194 2008). The primary sources of NBO include VOCs and NO_x emitted by natural sources such as vegetation, 195 soil, lightning, wildfires, and the oxidation of CH₄, as well as O₃ exchange between the stratosphere and 196 troposphere (Thompson, 2019). Historically, research into NBO originated with studies on atmospheric 197 photochemistry. In the 1950s, investigations into photochemical smog in Los Angeles identified O3 as a 198 major component of smog, linking vehicular emissions of VOCs and NOx to its formation (Haagen-Smit, 199 1952). While these studies primarily focused on anthropogenic sources, they also observed detectable O₃ 200 concentrations in remote regions, far from urban pollution, suggesting natural processes contributed to 201 O₃ production (Galbally et al., 1986; Volz and Kley, 1988). By the late 1970s, systematic studies in the 202 United States identified key natural sources of O₃, such as biogenic VOCs (BVOCs), lightning, and soil-203 emitted NO_x, leading to the formation of the NBO concept (Crutzen, 1974; Jacob et al., 1999; Liu et al., 204 1987). Although NBO holds significant scientific importance, its practical application as a regulatory 205 tool remains limited, particularly in the Northern Hemisphere, where anthropogenic emissions dominate 206 regional O₃ production (Berlin et al., 2013). Nonetheless, NBO is a critical reference for establishing 207 baseline O₃ levels globally, facilitating the evaluation of human contribution to atmospheric O₃ 208 concentration. 209 In the 1990s, researchers in the United States began to recognize the critical role of long-range 210 transport from anthropogenic sources in regional O₃ levels (Fiore et al., 2002a; Jacob et al., 1999; 211 Vingarzan, 2004). This realization was pivotal in developing the concept of United States Background 212 Ozone (USBO), which includes O3 contributions from global NBO as well as anthropogenic emissions 213 originating outside the country, such as from neighboring regions like Canada and Mexico (Skipper et 214 al., 2021; Thompson, 2019). Acknowledging these external sources highlighted that background O₃ 215 levels could not be fully mitigated through domestic emission reductions alone. 216 By the early 21st century, research on background O₃ increasingly intersected with air quality policy

218

219

220

221

222

223

224

225

226

227

228

229

230

231

232

233

234

235

236

237

238

239

240

241

242

243





development. A notable milestone was the introduction of Policy Relevant Background Ozone (PRBO) by the United States Environmental Protection Agency (EPA) in 2006 during revisions to the National Ambient Air Quality Standards (NAAQS) (U.S. EPA, 2006; Zhang et al., 2011). PRBO refers to groundlevel O3 concentrations that exclude all anthropogenic emissions from North America (the United States, Canada and Mexico) while accounting for natural sources and long-range transport from anthropogenic and natural sources outside North America (Emery et al., 2012; Nopmongcol et al., 2016). This concept aimed to help policymakers assess the effectiveness of domestic control measures in reducing O₃ pollution and inform the establishment of stricter O₃ standards. By differentiating controllable from uncontrollable O3 sources, PRBO enabled a more targeted approach to air quality management, framing policy discussions around the limitations of local pollution control in addressing O3 levels (Duc et al., 2013; Zhang et al., 2011). The introduction of PRBO marked a significant transition in background O₃ research, shifting from a predominantly scientific focus to one directly informing air quality policy and regulatory frameworks (Hosseinpour et al., 2024; U.S. EPA, 2006, 2007). Although USBO and PRBO share some common elements, their definitions differ primarily in geographic scope. PRBO focuses on transboundary contributions from regions outside North America, whereas USBO includes emissions from neighboring countries, such as Canada and Mexico, that affect the United States O₃ concentration. To address regional variations and better capture the dynamic of background O₃ in specific areas, advancements in atmospheric chemistry models have enabled scientists to differentiate the contributions of various sources to background O₃. This led to the emergence and widespread adoption of the term Regional Background Ozone (RBO) around the 2010s (Kemball-Cook et al., 2009; Langford et al., 2009; Ou-Yang et al., 2013). RBO refers to O3 concentrations within a defined region that are unaffected by direct local anthropogenic emissions. Its main sources include natural emissions (e.g., BVOCs, soil, wildfires, and lightning), the oxidation of CH₄, stratospherictropospheric exchange, and long-range transport (McDonald-Buller et al., 2011; Skipper et al., 2021; Sun et al., 2024; Wang et al., 2022). The distinction between NBO and RBO is crucial for understanding the complexity of background O3 concentrations, as each reflects different sources and scales of influence. NBO represents a natural





baseline, dominated by non-anthropogenic factors, serving as a reference point for assessing the human impact on atmospheric composition. In contrast, RBO reflects the interplay of natural and anthropogenic sources at local and global scales. Advancing our understanding of both NBO and RBO is essential for improving air quality models, refining emission control strategies, and establishing science-based standards for O₃ pollution reduction.

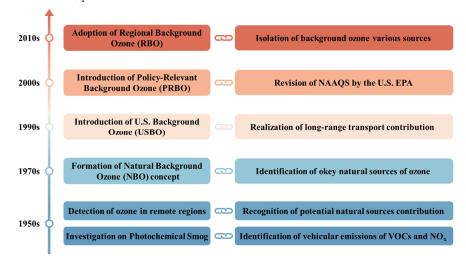


Figure 2: The evolution of background O₃ definitions.

4 Methods for estimating background ozone concentrations

The estimation of regional background O₃ is typically conducted using four primary methods: (1) in situ measurement estimation, (2) statistical analysis estimation, (3) numerical modeling estimation, and (4) integrated method estimation. Figure 3 summarizes the advantages, limitations, and applicability of each method, providing a comparative overview of their respective strengths and weaknesses.

4.1 In situ measurement estimation

The in situ measurement estimation method involves the deployment of monitoring stations in remote or elevated areas, typically located far from direct pollution sources, to measure O₃ concentrations directly (Lam and Cheung, 2022; Wang et al., 2009b). This approach is widely recognized as one of the most direct and commonly used methods for estimating regional background O₃. It is relatively straightforward





261 to implement, requires minimal post-measurement processing, and provides continuous, high frequency 262 data on O₃ variations across spatial and temporal scales. These attributes render it an invaluable tool for 263 tracking long-term trends in background O3 concentrations. 264 However, this method has limitations, particularly concerning the spatial representativeness of the 265 data. The limited number of monitoring stations, especially in regions with complex terrain or vast 266 geographic areas, can result in insufficient coverage of the region's environmental conditions. 267 Furthermore, measurements from background stations are subject to local meteorological conditions, 268 such as temperature, humidity, and wind patterns, which can introduce uncertainties into background O3 269 concentrations estimates (Skipper et al., 2021; Wu et al., 2017). This challenge is particularly pronounced 270 in the Northern Hemisphere, where widespread anthropogenic emissions complicate the identification of 271 truly "background" stations that are unaffected by human activities (Cooper et al., 2012; McDonald-272 Buller et al., 2011; Skipper et al., 2021; Vingarzan, 2004). 273 Despite its limitations, the in situ measurement estimation method remains an indispensable tool 274 for estimating background O3 concentrations. For instance, Vingarzan (2004) reported that background 275 O₃ concentration in the Northern Hemisphere rose from approximately 10 ppb before the Industrial 276 Revolution to 25-40 ppb by the 2000s, corresponding to an annual growth rate of 0.5-2 %. Similarly, 277 Akimoto et al. (2015) found background O₃ concentrations ranging from 60 to 70 ppb in Japan's Tokyo 278 and Fukuoka metropolitan areas between 1990 and 2008. In southern China, Wang et al. (2009b) recorded 279 background O₃ levels of 30-40 ppb at the Hok Tsui station in Hong Kong from 1994 to 2018, with an 280 average annual increment of 0.58 ppb. These studies demonstrate that, despite challenges in achieving 281 complete representativeness, the in situ measurement estimation method provides valuable insights into 282 regional background O3 trends and advances our understanding of the long-term impacts of both natural 283 and anthropogenic processes on atmospheric chemistry. 284 4.2 Statistical analysis estimation 285 The statistical analysis estimation method uses observed O₃ concentration data and applies statistical 286 techniques to estimate regional background O3 levels (Altshuller and Lefohn, 1996; Berlin et al., 2013;

Steiner et al., 2010; Wang et al., 2022). Historically, such estimations primarily relied on real-time





measurements from monitoring stations. However, limitations in the spatial and temporal coverage of monitoring networks, along with their susceptibility to local environmental factors, have constrained their ability to capture the broader regional O₃ levels accurately. For example, monitoring stations situated in areas with complex terrain may yield skewed data due to topographical effects on air circulation patterns, which in turn significantly influence the distribution of O₃ concentration (Wang et al., 2022). To overcome these challenges, researchers have increasingly adopted advanced statistical models that incorporate diverse observational data sources, enhancing the accuracy and reliability of background O₃ estimates (Riley et al., 2023; Rizos et al., 2022).

A notable advantage of statistical analysis estimation methods is their capability to process extensive datasets over long temporal scales, providing a cost-effective approach to estimating regional background O₃ levels. These methods can leverage large-scale data networks, such as satellite observations or regional monitoring systems (Langford et al., 2009). However, the reliability of statistical models is heavily dependent on the quality and spatial representativeness of the input observational data. High quality data are essential to minimize biases, and the monitoring stations must be strategically distributed to represent the target region adequately. Additionally, rigorous data preprocessing is critical to mitigate the influence of external factors, such as extreme weather events, that may distort the background O₃ concentrations estimates (Berlin et al., 2013; Langford et al., 2009).

The commonly used statistical analysis methods include the following:

4.2.1 Principal Component Analysis

Principal Component Analysis (PCA) is a widely used multivariate statistical technique designed to extract key patterns from datasets containing multiple interrelated variables (Jolliffe, 2005). By transforming correlated variables into a smaller set of uncorrelated principal components, PCA effectively reduces data complexity while preserving the most significant information. In the context of atmospheric pollution, PCA has proven to be particularly useful for isolating background O₃ by minimizing the influences from meteorological factors, such as temperature, humidity, and wind, as well as local airflows from urban and industrial sources. This makes PCA an invaluable tool for understanding regional air quality and estimating background O₃ levels, particularly in cases where direct measurements





are confounded by local pollution or short-term meteorological variability.

Despite its effectiveness, the application of PCA requires substantial computational resources, particularly when processing large datasets with high temporal and spatial resolution. Additionally, the accuracy of PCA results is highly contingent upon the availability of high-quality, long-term observational data. As emphasized by Wang et al. (2022), insufficiently robust datasets can hinder PCA's ability to isolate the true background O₃ signal, resulting in biased or unreliable estimates.

Langford et al. (2009) applied PCA to analyze regional background O₃ concentrations in Texas from August to October 2006. Their analysis revealed that the first principal component accounted for approximately 84 % of the variance in the O₃ data, strongly indicating its relevance as a proxy for background O₃ levels. The estimated background O₃ concentrations at monitoring stations across Texas ranged from 15 to 75 ppb, with higher values typically observed in rural areas with minimal local pollution. Similarly, Suciu et al. (2017) and Berlin et al. (2013) employed PCA to estimate background O₃ levels in Houston, Texas, reporting concentrations between 29 and 50 ppb. In China, Liang et al. (2018) and Wang et al. (2022) applied PCA to estimate background O₃ concentrations, which ranged from 35 to 70 ppb in the Yangtze River Delta region in May 2016 and from 30 to 75 ppb in Shandong Province between 2018 and 2020. These findings underscore the robustness of PCA in estimating background O₃ levels and highlight its versatility across diverse geographical regions, including both developed and developing regions worldwide.

4.2.2 K-means clustering

K-means clustering is an unsupervised, iterative machine-learning algorithm widely employed for grouping data, such as O₃ concentrations, meteorological parameters, and other environmental factors, based on shared characteristics (Riley et al., 2023). Its primary strength lies in the ability to discern patterns within large and complex datasets by clustering observations with similar attributes. Clusters with minimal anthropogenic influence are often interpreted as representative of background O₃ concentrations. These clusters, typically defined by low pollutant levels or specific meteorological conditions, facilitate the identification of periods or locations where regional background O₃ can be reliably assessed (Riley et al., 2023; Zohdirad et al., 2022).





The computational efficiency of K-means clustering makes it particularly suitable for large-scale studies, as it can simultaneously analyze multiple variables influencing O₃ variability, such as temperature, humidity, and wind patterns. This capability to manage multivariate data enables K-means to derive meaningful insights from complex datasets, which is especially useful in evaluating background O₃ in regions with diverse environmental conditions. For example, Riley et al. (2023) applied K-means clustering to estimate background O₃ concentrations in eastern Australia from 2017 to 2022. Their analysis revealed an average background O₃ concentration of 28.5 ppb, with a decadal increase of 1.8 ppb, reflecting the global trend of rising background O₃ levels.

Despite its utility, the effectiveness of K-means clustering is highly dependent on the quality of input data. The algorithm is sensitive to noise, outliers, and inconsistencies, which can undermine the

input data. The algorithm is sensitive to noise, outliers, and inconsistencies, which can undermine the reliability of its results. For example, extreme weather events or episodic pollution spikes can distort the clustering process, leading to inaccurate estimations of background O₃. Consequently, high-quality, well-preprocessed datasets are essential to ensure robust and reliable outcomes. Furthermore, K-means clustering is a descriptive rather than a causa technique, meaning it identifies associations between variables but does not elucidate the underlying physical or chemical mechanisms of O₃ formation (Govender and Sivakumar, 2020; Ning et al., 2024; Riley et al., 2023). To mitigate these limitations and enhance the accuracy of background O₃ estimates, K-means clustering can be integrated with other complementary analytical methods, combining its descriptive power with approaches that provide deeper causal understanding (Riley et al., 2023).

4.2.3 TCEQ method

The Texas Commission on Environmental Quality (TCEQ) method, based on O₃ monitoring data from background regions, has been widely adopted in Texas, the United States, as a reliable approach for estimating regional background O₃ levels (Nielsen-Gammon et al., 2005). This approach defines regional background O₃ as the minimum value within the maximum daily 8-hour average (MDA8) O₃ across all monitoring stations in a given area, effectively representing the lowest O₃ levels unaffected by local emissions (Wu et al., 2017). By focusing on these minimum values over an extended period, the TCEQ method isolates background concentrations, which are crucial for understanding regional air quality and

370

371

372

373

374

375

376

377

378

379

380

381

382

383

384

385

386

387

388

389

390

391

392

393

394

395





evaluating long-term trends in O₃ pollution.

Compared to more complex statistical methods such as PCA, the TCEQ method is simpler to implement and often yields more consistent and interpretable results. However, it is not without limitations. The method is sensitive to meteorological variability, which can lead to temporary spikes or drops in O₃ concentrations, potentially affecting accuracy. Additionally, the TCEQ method requires a dense network of monitoring stations to accurately represent regional background O3 levels, as sparse monitoring coverage may fail to capture true background concentrations (Wang et al., 2022; Wu et al., 2017). Despite these limitations, the TCEQ method has provided valuable insights into background O₃ levels across various regions. For instance, Berlin et al. (2013) and Langford et al. (2009) used this method to estimate background O₃ concentrations during high-O₃ periods (May-October) in Texas between 2000 and 2012. Their estimates ranged from 25 to 45 ppb and 40 to 80 ppb, respectively. Beyond the United States, the TCEQ method has been applied in diverse geographical regions, further underscoring its utility. For example, Xue et al. (2014) applied the TCEQ method to estimate background O_x (O₃ + NO₂) concentrations in Hong Kong from 2002 to 2013, reporting an average O_x concentration of 54 ppb with an annual increase of 0.52 ± 0.55 ppb yr⁻¹, highlighting the growing trend of background O₃ pollution in urbanized regions of Asia. Similarly, Wang et al. (2022) estimated background O₃ concentrations in Shandong Province, China, to average 31.4 ppb from 2018 to 2020. These findings demonstrate that the TCEQ method is adaptable across different geographical contexts and provides

4.2.4 O₃-NO_z intercept method

The O₃-NO_z intercept method is an approach for estimating background O₃ concentrations by establishing the linear relationship between O₃ concentrations and its precursors (Altshuller and Lefohn, 1996; Hirsch et al., 1996; Yan et al., 2021). In this approach, NO_z is defined as the difference between NO_y (the total reactive nitrogen species, including nitric acid and peroxy nitrates) and NO_x (which comprises NO and NO₂). NO_z serves as an indirect indicator of background O₃ level, based on the assumption that it reflects the presence of O₃-producing precursors in the atmosphere. Through

robust background O3 estimates that can inform air quality management strategies and policymaking.





396 regression analysis, O3 levels are extrapolated to the intercept where NOz equals zero, representing an 397 approximation of background O3 concentrations unaffected by local emissions and photochemical 398 influences. 399 One of the key strengths of this method lies in its simplicity, as it requires only reliable 400 measurements of O₃, NO_x, and NO_y without necessitating extensive observational networks. However, 401 the method's validity depends heavily on the assumption of a linear relationship between O₃ and NO_z, 402 which may not hold under all atmospheric conditions. For instance, photochemical processes, such as 403 the formation of secondary pollutants, meteorological variability (e.g., wind, temperature), and local 404 environmental factors can introduce non-linearities into the O₃-NO_z relationship, potentially impacting 405 the accuracy of the estimates. Additionally, the method's precision is highly sensitive to the quality of 406 O₃, NO_x, and NO_y measurements, as inaccuracies in these data can result in significant biases when 407 estimating background O3 levels. 408 Several studies have applied the O₃-NO₂ intercept method to estimate background O₃ concentrations 409 in various regions, providing valuable insights into its efficacy and limitations. For example, Hirsch et 410 al. (1996) applied this method at Harvard Forest in the United States, estimating background O₃ 411 concentrations of 40 ppb in May and 25 ppb in September. Similarly, Yan et al. (2021) applied the method 412 in the southeastern United States during the summer of 2013, estimating background O₃ concentrations 413 of 29.8 ppb in a region influenced by both local emissions and regional transport of pollutants. However, 414 Yan et al. (2021) noted that the method's accuracy could be compromised in areas with high rates of 415 nitric acid (HNO₃) deposition. Elevated HNO₃ deposition sequesters reactive nitrogen compounds at the 416 surface, potentially masking near-surface O3 levels and leading to overestimations of background O3 417 concentrations. 418 To address these limitations, Yan et al. (2021) proposed a modified version of the O₃-NO_z method, 419 referred to as the 1-σ O₃-NO_z method. This refinement involved excluding regions with high HNO₃ 420 deposition rates and minimizing the influence of regional emissions through improved data selection 421 criteria. The modified method estimated background O₃ concentration at 21.3 ppb, approximately 8 ppb 422 lower than the traditional O3-NOz method, demonstrating enhanced reliability under conditions with





- 423 elevated nitrogen deposition. This modification highlights the importance of accounting for nitrogen
- deposition dynamics to improve the robustness of background O₃ estimations.

425 4.2.5 O₃-CO-HCHO response method

- 426 Cheng et al. (2018) introduced an innovative approach for estimating background O₃ concentrations by
- 427 using carbon monoxide (CO) and formaldehyde (HCHO) as chemical indicators to trace the production
- 428 and consumption of O₃. This method integrates the chemical reaction dynamics between O₃, CO, and
- 429 HCHO, resulting in a rapid-response O₃ estimator. This approach was specifically designed to enhance
- 430 the efficiency and accuracy of O₃ estimation by leveraging the dynamic chemical processes that influence
- 431 O₃ levels. Building upon this foundation, Yan et al. (2021) proposed the O₃-CO-HCHO approach, which
- 432 refines the original concept by eliminating the influence of both anthropogenic and natural emissions of
- 433 O₃ precursors, enabling a more accurate estimation of background O₃ concentrations.
- The O₃-CO-HCHO method is particularly advantageous due to its applicability to both
- data and model outputs, offering robust results across a broad range of conditions. The
- 436 method is governed by the following key equations:

437
$$O_3 = k_1(CO_{total} - CO_{back}) - (k_1k_2 - k_3)(HCHO_{total} - HCHO_{back}) + O_{3back},$$
(2)

438
$$O_{3back} = O_3 - k_1(CO_{total} - CO_{back}) + (k_1k_2 - k_3)(HCHO_{total} - HCHO_{back}),$$
 (3)

- Here, $k_1 = \frac{\Delta O_3}{\Delta CO_{anthro}}$, $k_2 = \frac{\Delta CO_{bio}}{\Delta HCHO_{bio}}$, $k_3 = \frac{\Delta O_3}{\Delta HCHO_{bio}}$. The terms "anthro", "bio", "total", and
- 440 "back" refer to anthropogenic sources, biogenic sources, total sources, and background sources,
- 441 respectively.
- In model-based applications, tracer simulations provide the necessary inputs to determine the
- unknown variables on the right-hand side of Eq. (3), facilitating the estimation of background O₃
- 444 concentrations. This capability makes the method particularly valuable in model-based studies, where
- 445 emissions sources and their contributions are explicitly tracked. Conversely, when applied to
- observational data, distinguishing the origins of various species presents challenges. Empirical methods
- 447 can be employed to approximate missing variables, combining observational data with nonlinear
- 448 regression analysis, as described in Eq. (2). This enables the estimation of background O₃ concentrations





even in the absence of precise source-specific information.

However, it is important to note that the chemical interactions among O₃, CO, and HCHO are inherently nonlinear and influenced by regional geography, meteorological conditions, and other environmental factors. These complexities may limit the method's accuracy, as its performance is highly context dependent. (Cheng et al., 2018; Yan et al., 2021). Specifically, the current methodology is most effective in regions minimally affected by anthropogenic pollution, where HCHO is primarily formed via the oxidation of biogenic isoprene, such as in the southeastern United States. A limitation of this method is the difficulty of disentangling contributions from natural and anthropogenic O₃ precursors. Nevertheless, Yan et al. (2021) proposed integrating the O₃-CO-HCHO method with an "anthropogenic-source-zeroing" scenario, which can estimate the impact of emissions from natural sources.

Applying the O₃-CO-HCHO method, Yan et al. (2021) estimated the background O₃ concentration in the inland regions of the southeastern United States during the summer of 2013 to range between 10-15 ppb, approximately 5-10 ppb lower than estimates derived from other methods. This refinement highlights the utility of the O₃-CO-HCHO method for achieving more accurate assessments of zero-chemical-signature background O₃ concentrations.

4.2.6 Percentile method

The percentile method is a widely adopted statistical analysis estimation approach for estimating regional background O₃ concentrations, offering a straightforward and practical alternative to complex modeling techniques (Berlin et al., 2013; Jenkin, 2008). This method involves analyzing O₃ concentration data over a specific time period and selecting a particular percentile to represent the background O₃ levels. The selected percentile is assumed to reflect minimal O₃ concentrations that are largely unaffected by local pollution sources, thereby serving as a proxy for regional background O₃ concentrations.

A key advantage of the percentile method lies in its simplicity and ease of implementation, making it particularly suitable for regions with limited monitoring networks or computational resources required for advanced modeling techniques. However, the reliability and accuracy of this method are highly dependent on the selection of the appropriate percentile value, which can vary significantly depending on regional characteristics such as emissions patterns, meteorological conditions, and topographical





features (Cooper et al., 2012). Consequently, the chosen percentile may exhibit significant variability across different geographical regions, potentially affecting the consistency of background O₃ estimates. For example, Akimoto et al. (2015) proposed using the 2nd percentile of MDA8 O₃ concentrations as a suitable measure of background O₃ levels in Japan, capturing low concentrations unaffected by local anthropogenic emissions during high-O₃ episodes. In contrast, Yan et al. (2021) applied the 5th percentile to estimate background O₃ concentrations in the southeastern United States. Similarly, Cooper et al. (2012) and Wilson et al. (2012) advocated for the use of the 5th percentile in their studies of background O₃ levels in the United States and Europe, respectively, suggesting it achieves a balance between accurately representing background O₃ levels and accounting for regional variations in pollutant emissions.

4.2.7 Temperature-ozone relationship method

The temperature-ozone relationship method estimates background O₃ contributions by analyzing the correlation between O₃ concentrations and temperature (Mahmud et al., 2008). Generally, O₃ concentrations increase with rising temperatures, as elevated temperatures enhance the photochemical reactions that produce O₃. However, within a specific temperature range, O₃ concentrations tend to stabilize due to the equilibrium between O₃ production and destruction processes. These stabilized O₃ levels, typically observed during periods of relatively stable meteorological conditions, are often regarded as indicative of regional background O₃ concentrations, reflecting natural influence rather than anthropogenic emissions (Mahmud et al., 2008; Sillman and Samson, 1995; Steiner et al., 2010).

This method offers several advantages, primarily its simplicity and reliance on widely available observational meteorological and O₃ concentrations data. Given the accessibility of temperature datasets, the temperature-ozone relationship method is particularly effective for conducting large-scale spatial and temporal analyses. Its versatility is demonstrated by its applicability across diverse geographic regions and climatic conditions, ranging from temperate zones to tropical climates, where temperature plays a key role in driving O₃ dynamics.

Despite its practicality, the method has certain limitations. A primary challenge is the variability in the temperature range corresponding to stable O₃ levels, which differs among regions due to local





meteorological and geographical factors. Extreme meteorological conditions, such as high humidity or strong winds, can disrupt the temperature-ozone correlation, reducing the reliability of this method in such scenarios. Moreover, O₃ formation is influenced by multiple factors, including solar radiation, precursor emissions, and atmospheric chemistry, making temperature an incomplete predictor of O₃ dynamics. The method's accuracy also depends on the quality and temporal resolution of the data used; short-term datasets, such as those based on monthly averages, can introduce significant uncertainties due to O₃'s sensitivity to short-term meteorological fluctuations and emission variations. This limitation underscores the importance of using long-term, high-resolution datasets to derive more reliable temperature-ozone relationships (Li et al., 2020; Liao et al., 2021). Incorporating seasonal and regional variations in temperature and O₃ formation processes can further enhance the method's accuracy.

Despite these challenges, the temperature-ozone relationship method has been successfully applied in several studies to estimate background O₃ concentrations. For example, Steiner et al. (2010) applied this method to estimate the average background O₃ concentrations in California during the summer months (June-October) between 1980 and 2005, finding values ranging from 30 to 40 ppb. Similarly, Chen et al. (2022) used this method to assess background O₃ levels in China from 2013 to 2019, reporting concentrations of 35-40 ppb during clean seasons and 50-55 ppb during O₃-polluted seasons.

4.2.8 Nocturnal ozone concentration method

The nocturnal O₃ concentration method leverages the relatively stable O₃ levels observed during nighttime, when photochemical reactions driven by sunlight are absent, making it a valuable approach for estimating regional background O₃ levels (Chan et al., 2003). At night, O₃ levels generally remain constant or exhibit minimal fluctuations, as they are primarily governed by the equilibrium between O₃ production and destruction through reactions with NO_x and other atmospheric components. However, this method is not without its challenges. A key limitation arises from the titration reaction between O₃ and NO, which produces NO₂ and depletes ambient O₃ levels. This phenomenon, known as O₃ titration, can result in underestimation of true background O₃ concentrations, particularly in areas with elevated NO emissions (Akimoto et al., 2015; Itano et al., 2007; Shin et al., 2012).

To mitigate the impact of O₃ titration, researchers have introduced adjustments to nocturnal O₃

538

544

546

547

548

549

550

551

552

553

554

555

556





estimates by incorporating a "total O_3 " concentration, denoted as O_{3total} , which serves as a proxy for

background O₃ levels. The "total O₃" is calculated using the following equations:

532
$$\left[O_{3_{\text{total}}}\right] = \left[O_{3}\right] + \left[NO_{2}\right] - \alpha \times \left[NO_{x}\right],$$
 (4)

Here, $[O_3]$, $[NO_2]$, and $[NO_x]$ (= $[NO] + [NO_2]$) represent the mixing ratios of O_3 , NO_2 , and NO_x ,

534 respectively. The parameter α accounts for the fraction of NO₂ in NO₃ from primary emissions, with a

535 typical value of $\alpha = 0.1$ used in most studies (Akimoto et al., 2015; Itano et al., 2007; Shin et al., 2012).

536 However, Wang et al. (2009b) suggested a lower value of $\alpha = 0.041$, introducing variability in the

estimated $[0_{3}]$. This adjustment helps to compensate for the effects of NO titration, yielding a more

accurate representation of regional background O3 levels.

Despite its utility, the nocturnal O₃ concentration method is subject to inherent limitations. A

540 primary drawback is its reliance on observational data, which can be influenced by local variations in

emissions and meteorological conditions, thereby complicating the estimation process.

542 In an applied context, Chen et al. (2022) used the nocturnal O₃ concentration method to estimate

background O₃ levels across China during the period from 2013 to 2019. Their analysis revealed that

background O₃ concentrations ranged between 25 and 38 ppb during clean seasons and between 35 and

545 49 ppb during O₃-polluted seasons.

4.3 Numerical modeling estimation

The numerical modeling estimation method, which uses atmospheric chemistry and transport models such as GEOS-Chem, WRF-Chem, and CMAQ, is widely employed to simulate the formation, transportation, and variability of regional background O₃ concentrations. These models offer several distinct advantages by incorporating a comprehensive array of atmospheric processes, including photochemical reactions, vertical mixing, advection, and the transport of pollutants across various spatial and temporal scales. By accounting for the intricate interactions among emissions, meteorological conditions, and atmospheric chemistry, numerical models provide a more robust and accurate representation of regional background O₃ levels compared to in situ measurement estimation or statistical analysis estimation methods alone. Additionally, numerical models can be customized to align with specific research objectives through adjustments to chemical mechanisms and parameterization schemes,

558

559

560

561

562

563

564

565

566

567

568

569

570

571

572

573

574

575

576

577

578

579

580

581

582

583





rendering them adaptable to diverse regions and temporal scales.

A notable strength of numerical models lies in their ability to differentiate the contributions of various emission sources to regional O₃ concentrations (Jaffe et al., 2018; Thompson, 2019; Zhang et al., 2011). This capability sets them apart from in situ measurement estimation and statistical analysis estimation approaches, which typically lack the granularity to isolate the relative contributions of natural versus anthropogenic emissions. However, numerical modeling estimation also presents significant challenges. These models are computationally intensive, requiring substantial resources, especially when simulating extensive domains or prolonged time periods. Moreover, their accuracy depends heavily on the quality of input data, such as emission inventories, meteorological conditions, and assumptions regarding physical and chemical processes, which can introduce uncertainties in estimated O₃ concentrations (Dolwick et al., 2015; Guo et al., 2018; Hogrefe et al., 2018; Jaffe et al., 2018). Numerical models typically estimate regional background O3 concentrations using two primary approaches: the emission scenario method and the tracer method (Fiore et al., 2002a). The emission scenario method employs three-dimensional air quality models, such as GEOS-Chem, MOZART, WRF-Chem, and CMAQ, to simulate background O3 levels by conducting perturbation experiments where local anthropogenic emissions are reduced or set to predefined values. This approach enables the isolation of local emissions' contributions to regional background O3 levels (Zhang et al., 2011; Li et al., 2018; Lu et al., 2019; Pfister et al., 2013). In contrast, the tracer method uses chemical tracers to track the transport and transformation of emissions, offering an alternative approach to estimating background O₃ concentrations. Models such as CMAQ-ISAM and CAMx-OSAT, developed by the United States Environmental Protection Agency (EPA), incorporate tracer methods to estimate regional background O₃ concentrations (Lefohn et al., 2014; Li et al., 2012; Reid et al., 2008). Although both methods have their strengths, studies have highlighted discrepancies in O3 estimates depending on the approach employed (Jaffe et al., 2018; Skipper et al., 2021). For example, Emery et al. (2012) found that the CAMx model generally produced higher background O₃ concentrations in the United States compared to GEOS-Chem, with CAMx showing a higher correlation with observational

data, especially at remote stations and during high-O3 episodes. Conversely, GEOS-Chem demonstrated

585

586

587

588

589

590

591

592

593

594

595

596

597

598

599

600

601

602

603

604

605

606

607

608

609

610





greater accuracy in capturing seasonal mean O3 concentrations in rural areas. Similarly, Dolwick et al. (2015) compared the tracer and emission scenario methods using CAMx and CMAQ models. Their analysis revealed consistent estimates of background O3 concentrations in suburban United States areas across both methods. However, in urban areas, the tracer method yielded lower background O3 estimates than the emission scenario method, indicating a substantial influence of local emissions on O₃ concentrations in densely populated regions. Equally, Fiore et al. (2014) reported differences in background O₃ concentrations between GEOS-Chem and GFDL-AM3 models, with variations ranging from 1 to 10 ppb depending on region, season, and altitude. Numerical modeling estimation has been extensively applied to estimate global and regional background O₃ concentrations. For example, using the global model GEOS-Chem, Emery et al. (2012) and Zhang et al. (2011) estimated average background O3 concentration in the United States from March to August 2006, ranging from 20 to 45 ppb, with 27 ± 8 ppb in low-altitude areas and 40 ± 7 ppb in highaltitude areas. Guo et al. (2018) reported annual variation of up to 15 ppb in regional background O₃ concentration in the United States between June and August from 2004 to 2012. Meanwhile, regional models such as CAMx and CMAQ yielded background O3 estimates of 25 to 50 ppb in the United States between March and August 2006 (Emery et al., 2012). In China, Sahu et al. (2021) found background O₃ concentrations exceeded 22 ppb in 2015. 4.4 Integrated method estimation The three methods discussed above each possess distinct advantages and limitations, contributing to uncertainties in estimating regional background O3 concentration. Given these challenges, researchers have increasingly turned to integrated method estimation methods to improve the accuracy and reliability of these estimations. For instance, Dolwick et al. (2015) improved model-based estimates of background O₃ by comparing observed and simulated O3 concentrations. Their analysis of rural areas in the western United States during April to October 2007 reported background O₃ concentrations ranging from 40 to 45 ppb, with the lowest concentrations observed along the Pacific coast, ranging from 25 to 35 ppb.

612

613

614

615

616

617

618

619

620

621

622

623

624

625

626

627

628

629

630

631

632

633

634

635

636

637





optimizing regional background O3 estimations. Based on this methodology, Skipper et al. (2021) extended the methodology by incorporating both spatial and temporal functions to account for variations driven by regional background O3 and anthropogenic emissions. This revised approach estimated an average background O₃ concentration of approximately 33 ppb for the United States in 2017, with peak values around 38 ppb. Notably, this adjustment improved the consistency of estimates by 28 % compared to the unadjusted model, demonstrating the utility of integrated method in refining atmospheric models. The rapid advancement of Machine Learning (ML) techniques has further facilitated the integration of these technologies with traditional methods for estimating regional background O3 concentrations. For example, Hosseinpour et al. (2024) developed a Multivariate Linear Regression (MVLR) model and a Random Forest (RF) based ML algorithm to adjust model-derived background O3 concentrations. While the MVLR model follows an adjustment method akin to that of Skipper et al. (2021), the RF-ML algorithm employs the Shapley Additive Explanations (SHAP) method to evaluate the relative importance of each input variable. The RF-ML model, trained using k-fold cross-validation, demonstrated superior predictive accuracy. Hosseinpour et al. (2024) showed that the RF-ML algorithm produced results most consistent with those from the in situ measurement estimation method, outperforming those from the original CAMx model, MVLR adjustments, and two other ML algorithms. Utilizing this methodology, they estimated background O₃ concentrations in 13 urban areas of the United States during April-June and July-September 2016 to range from 31-46 ppb and 27-45 ppb, respectively. This finding underscore the potential of ML algorithms to enhance model-based background O₃ estimates by capturing nonlinear relationships and complex variable interactions (Breiman, 2001; Kashinath et al., 2021). Overall, integrated method estimation methods, particularly those integrated with machine learning techniques, represent a significant advancement in estimating regional background O₃ concentrations. These approaches not only improve the accuracy and robustness of estimates but also provide valuable insights into the complex dynamics of O₃ formation and transport. By combining observational data, statistical adjustments, and advanced modeling techniques, researchers can achieve a more comprehensive understanding of regional O₃ levels and their temporal variations.





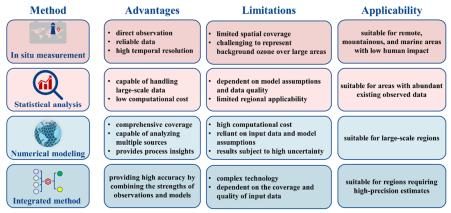


Figure 3: Summary of the advantages, limitations, and applicability of different estimation methods for background O₃.

5 Comprehensive assessment of background ozone in China: patterns, trends, sources, and global comparisons

5.1 Regional patterns of background ozone in China

Figure 4 presents the average background O_3 concentrations across China and its various regions. On a national scale, the average background O_3 concentration is 40.3 ± 11.9 ppb, accounting for 77 % of the MDA8 O_3 concentration. Notable regional variability in background O_3 concentrations is observed, highlighting the differential impacts of local meteorological conditions, pollutant emissions, and geographic characteristics.

Among the regions, Northwest China (NWC) stands out with the highest background O₃ concentrations, reaching 48.2 ± 8.3 ppb, which accounts for 96 % of the MDA8 O₃ concentration. This elevated concentration is attributed to several interrelated factors. First, strong solar radiation and arid atmospheric conditions enhance photochemical reactions, accelerating O₃ formation. He et al. (2021) demonstrated that abundant sunshine and dry conditions significantly increase O₃ production due to the intensified photolysis of precursor compounds. Furthermore, the high altitude and unique surface characteristics of Northwest China promote strong daytime atmospheric convection, facilitating the downward transport of O₃ from the upper atmosphere to the surface levels (Ding and Wang, 2006; Liu et al., 2019; Ma et al., 2005; Nie et al., 2004). Additionally, the relatively low anthropogenic emissions

659

660

661

662

663

664

665

666667

668

669

670

671

672

673

674

675

676

677

678

679

680

681

682

683

684





result in fewer precursors like NOx and VOCs, thereby minimizing rapid fluctuations in O3 levels. The weaker nocturnal O3 depletion, caused by limited O3 scavenging from sparse emissions and lower nighttime temperatures, further amplifies baseline O₃ concentrations (Nie et al., 2004; Qin et al., 2023; Xu et al., 2020). Southwest China (SWC), alongside with the urban clusters of East China (EC) and North China (NC), also exhibits higher background O₃ concentrations, averaging 38.7 ± 10.8 ppb, 38.4 ± 13.0 ppb, and 37.7 ± 13.5 ppb, respectively. These concentrations account for 84 %, 66 %, and 71 % of the MDA8 O3 concentration in each respective region. In Southwest China, regional pollutant transport plays a significant role. During the spring, prevailing winds carry pollutants such as NOx and VOCs from Southeast Asia, intensifying local O₃ levels (Ye et al., 2024). Summer conditions - characterized by high humidity, elevated temperatures, and intense solar radiation - further amplify photochemical O₃ formation (Chen, 2020). The region's complex topography, including mountainous areas and plateaus, also contributes to localized O₃ accumulation. For instance, the Sichuan Basin, with its basin - like terrain, impedes air mass dispersion, leading to pollutants entrapment and prolonged O₃ buildup (Hu et al., 2019). In contrast, East China and North China are heavily influenced by high industrial and vehicular emissions, which release significant quantities of NOx and VOCs. The precursors undergo photochemical reactions under intense sunlight and elevated summer temperatures, resulting in higher O3 levels. Moreover, the East Asian Summer Monsoon (EASM) facilitates the transport of O₃ and its precursors from low-latitude regions, such as South China, to higher latitudes, exacerbating O₃ pollution during the monsoon season (Gao et al., 2005; Liu et al., 2019, 2021; Sun et al., 2016; Xu et al., 2011, 2020) The background O₃ concentrations in South China (SC), Central China (CC), and Northeast China (NEC) are relatively low compared to other regions of China, with values of 35.5 ± 8.0 ppb, 33.2 ± 10.9 ppb, and 33.0 ± 5.7 ppb, respectively. These concentrations account for 71 %, 57 %, and 67 % of the MDA8 O3 in each corresponding region. In South China, the relatively low background O3 concentrations can be primarily attributed to the frequent rainfall and high humidity, which facilitate the removal of O₃ precursors such as NO_x and VOCs, thereby suppressing O₃ formation (He et al., 2021). Although BVOCs emissions are relatively high in this region due to abundant vegetation and elevated

686

687

688

689

690

691

692

693

694

695

696

697

698

699

700

701

702

703





temperatures, their impact on O₃ formation is less pronounced compared to regions like North China. This is because anthropogenic emissions, such as vehicular exhaust and industrial discharges, typically amplify the contribution of BVOCs on O3 formation. In the absence of significant anthropogenic pollution, the role of BVOCs in O₃ formation remains relatively limited (Ye et al., 2024). Moreover, the mixed topography of South China, characterized by a combination of hilly terrain and plains, promotes air mixing and disperse O₃, preventing its prolonged accumulation at the surface (Wang et al., 2011). In Central China (CC), the lower background O3 concentrations are linked to the region's inland locations, which reduces its exposure to oceanic influences and transboundary pollutant transport. The absence of strong maritime airflow limits the import of O₃ precursors, while frequent rainfall during the warmer months helps remove these precursors from the atmosphere, further suppressing O3 formation (Sahu et al., 2021). Anthropogenic emissions, primarily from vehicular exhaust, industrial discharges, and solvent usage, constitute the dominant sources of O₃ in this region (Zeng et al., 2018). Consequently, the relative contribution of background O3 is lower, as anthropogenic emissions play a more substantial role in O₃ formation. The combination of moderate meteorological conditions and limited transport of O₃ precursors contributes to the observed lower background O₃ levels in Central China. In Northeast China, the lower background O₃ concentration can be attributed to a prolonged period of low temperature, which significantly reduces the rate of photochemical reaction. Additionally, the region experiences strong summer air convection and substantial precipitation, both of which further inhibit O₃ generation (Chen, 2024; Xu et al., 2020).



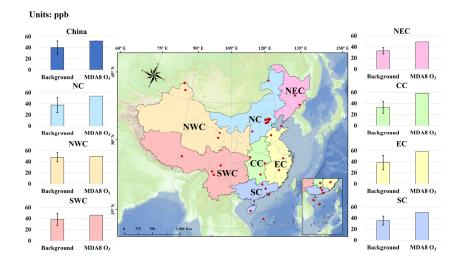


Figure 4: Spatial distribution of background O₃ concentrations (1994-2020) and MDA8 O₃ concentrations across various regions of China. MDA8 O₃ concentrations for the seven regions (2013 to 2018) were sourced from He et al. (2023). The locations of 33 background monitoring stations are indicated with red dots. The seven regions include Northeast China (NEC), North China (NC), East China (EC), Central China (CC), Northwest China (NWC), Southwest China (SWC), and South China (SC).

5.2 Comparative evaluation of background ozone concentration estimates using diverse methods

Figure 5 presents a comparison of average background O₃ concentrations across China, as estimated using various methods. Among these, the in situ measurement estimation method remains the most widely utilized, as it directly relies on observational data from established monitoring networks. In this study, data from 33 background monitoring stations were compiled (Fig. 4), with detailed information on their locations and characteristics provided in Table S3. In contrast, the other three methods, particularly the integrated method estimation approach, have been less frequently applied in research, reflecting their higher reliance on assumptions and advanced modeling techniques.

The estimated background O_3 concentrations for China derived from the four methods reveal relatively small differences in average values. The in situ measurement estimation method and statistical analysis estimation method yield the highest average concentration, with values of 40.6 ± 12.0 ppb and 39.9 ± 11.5 ppb, respectively, followed by the numerical modeling estimation method (36.5 ± 12.6 ppb). The integrated method estimation method, which integrates observational data with modeling outputs,

724

725

726

727

728

729

730

731

732

733

734

735

736

737

738

739

740

741

742

743

744

745

746

747

748

749





reports the lowest estimate (34.0 \pm 2.7 ppb), approximately 6 ppb lower than those from in situ measurement estimation and statistical analysis estimation methods.

Despite the similar average values, substantial discrepancies exist among the various methods used to estimate background O3 concentrations, underscoring the significant influence of methodological differences. The in situ measurement estimation reveals a particularly wide variability, with estimated background O₃ concentrations ranging from approximately 14 ppb to as high as 85 ppb. This broad range reflects the substantial influence of localized factors, such as topography, climatic conditions, and anthropogenic emissions, on observational data. In comparison, statistical analysis estimation and numerical modeling estimation methods yield relatively consistent results, although the difference between the maximum and minimum estimated background O3 concentration for both methods reach 60 ppb. Notably, more than 80 % of the estimated background O₃ concentrations fall within the range of 25-53 ppb, suggesting a reasonable degree of agreement between the two methods. The consistency is likely attributable to the reliance on long-term data trends and calibrated algorithms, which effectively reduce the impact of extreme values while capturing broader patterns in O₃ behavior. The integrated method estimation method, by integrating observational data, statistical analysis, and numerical results, exhibits the least variability. Background O₃ estimates from this approach are confined to a narrower range of 28-39 ppb, reflecting its ability to reconcile the inherent variability in observational data with the structured consistency of numerical models. This reduced uncertainty enhances the method's reliability for both scientific research and policy applications.

These differences highlight the complexities and challenges associated with estimating background O₃ concentrations using diverse methodologies. The variability observed across methods arises from several key factors, including disparities in data sources, underlying assumptions, and the parameterization of physical and chemical processes (Jaffe et al., 2018; Skipper et al., 2021; Wang et al., 2022; Yan et al., 2021). For instance, the in situ measurement estimation method is directly influenced by local meteorological and emission conditions, while the numerical modeling estimation method is subject to uncertainties in simulating processes such as natural emissions, transboundary transport, and photochemical reactions. Although the integrated method estimation method benefits from leveraging





both observations and modeled outputs, it may introduce additional uncertainty through integration techniques and sensitivity to the input data quality.

The discrepancies among these methods emphasize the need for further refinement and rigorous cross-validation to improve the accuracy and reliability of background O₃ concentration estimates. Future efforts should prioritize the expansion and enhancement of observational networks, the refinement of model parameterization schemes, and the development of advanced integrated method frameworks. Such advancements are essential for narrowing the discrepancies among different estimation methods, providing consistent and reliable background O₃ estimates, and enabling more effective air quality management and policy formulation.

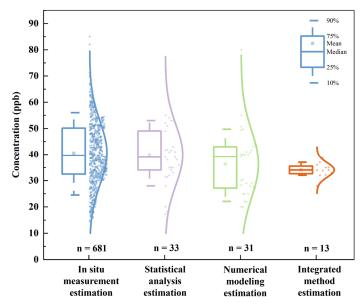


Figure 5: Estimated regional average background O₃ concentrations in China (1994-2020) based on multiple methods.

5.3 Long-term trends and interannual variability of background ozone in China

Due to the absence of long-term background O₃ concentration data for other regions, Figure 6 focuses on the annual variation trends of background O₃ concentrations in four major regions of China (i.e., NWC, NC, EC, and SC) during the period from 1994 to 2020. Overall, background O₃ concentrations in these regions have exhibited an upward trend over the years, albeit with notable differences in growth rates

768

769

770

771

772

773

774

775

776

777

778

779

780

781

782

783

784

785

786

787

788

789

790

791

792

793





across regions. Notably, Northwest China (NWC) exhibited the most pronounced increase in background O₃ concentration, with an average annual growth rate of 0.32 ppb yr⁻¹ (r²=0.68, p<0.01), as shown in Fig. 6(a). This marked growth is likely driven by the stratospheric-tropospheric exchange and regional transport of O₃ precursors, as suggested by Xu et al. (2018) and Zhang et al. (2020). Previous studies have highlighted the significant role of long-range transport of air pollutants in this region, contributing to elevated O3 levels. In addition, shifts in atmospheric circulation and an increase in the frequency of stratospheric-tropospheric exchange events further amplify O3 concentration in this region (Xu et al., 2016, 2020; Xue et al., 2011). Following, North China (NC) and East China (EC) also experienced notable increases in background O₃ concentration, each with an average annual growth rate of 0.26 ppb yr⁻¹, as shown in Fig. 6(b) and Fig. 6(c). However, a statistically significant upward trend was observed in North China, where the increase passed the 0.01 confidence level. In contrast, the growth rate in East China, though comparable, did not achieve statistical significance (p>0.05), suggesting regional variability in the factors driving O3 trends. This discrepancy could be attributed to differences in urbanization levels, industrialization intensity, and meteorological conditions, which modulate the dispersion and chemical transformation of O₃ precursors differently in these regions (Ma et al., 2016; Xu et al., 2020; Zhang et al., 2020). A detailed study by Ma et al. (2016) further supports these findings, reporting a higher growth rate in background O₃ concentration in North China, reaching 1 ppb yr⁻¹ (r²=0.58, p<0.01), based on data from the Shangdianzi background station. This finding highlights the intensification of regional background O₃ pollution, likely driven by both local emissions and the regional atmospheric conditions conducive to O3 accumulation. In stark contrast, South China (SC) experienced the slowest growth in background O₃ concentration, with an average annual increase of only 0.19 ppb yr⁻¹ (r²=0.21, p<0.05), as shown in Fig. 6(d). This relatively modest increase may be attributed to a combination of factors, including more stable natural and anthropogenic emission sources and more effective atmospheric cleansing processes (Qin et al., 2021;

Shen and Wang, 2012; Xie et al., 2022; Zhang and Zhang, 2019). For instance, the region's comparatively





higher precipitation rates and frequent weather systems facilitate the removal of pollutants from the atmosphere, thereby moderating O₃ levels.

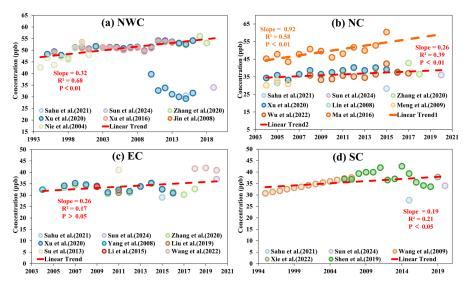


Figure 6: Annual trend of background O₃ concentrations in the NWC (1994-2019), NC (2004-2020), EC (2004-2020), and SC regions (1995-2020). The dashed lines represent the linear trends.

5.4 Source attribution and analysis of background ozone in China

The analysis above reveals that the growth characteristics of background O₃ concentrations across different regions of China are influenced by the synergistic effects of multiple factors, including regional natural source emissions, cross-regional transport, stratospheric-tropospheric exchange, and local atmospheric pollutant reduction measures. These factors interact in complex and dynamic ways, resulting in significant regional and seasonal variations in background O₃ levels.

Natural source emissions are a key driver of background O₃ levels in China, with studies consistently highlighting their substantial contribution. For example, Wang et al. (2011) and Lu et al. (2019), using the numerical model GEOS-Chem, estimated that over 70 % of regional background O₃ concentrations in China originate from natural emissions, including BVOCs, soil NO_x, and CH₄ emissions and others. Among these, BVOCs exert a particularly significant impact on O₃ formation. Lu et al. (2019) demonstrated that during the peak summer months of July and August in 2016-2017, BVOCs emissions contributed over 15 ppb to the background O₃ in central and eastern China. Similarly, Chen et





812 al. (2022) emphasized that during O₃ pollution seasons, BVOCs emissions dominate the increase in 813 background O₃, contributing 8-16 ppb compared to non-pollution seasons. These findings underscore the 814 importance of incorporating the variability of natural emissions into modeling and policy frameworks, 815 particularly in light of future climate change that may exacerbate BVOCs emissions. 816 Long-range transport plays an equally significant role in shaping background O3 concentration 817 across China. Several studies have shown that the influx of O₃ and its precursors from other regions, 818 including Southeast Asia, Europe, North America, India, and the Middle East, can elevate background 819 O₃ concentration in China by 2-15 ppb (Wang et al. (2011), Li et al. (2014), and Ni et al. (2018)). This 820 influence is particularly pronounced during specific seasons when atmospheric circulation facilitates the 821 transboundary transport of atmospheric pollutants (Ni et al., 2018; Sahu et al., 2021; Ye et al., 2024). 822 Regional transport also significantly influences the background O₃ levels in urbanized and densely 823 populated areas. For instance, Su et al. (2013) showed that air masses originating from high altitudes, the 824 Yangtze River Delta region, and the Pearl River Delta regions could cause spikes at the Mount Wuyi 825 background station, with concentration reaching 62-73 ppb, far exceeding the station's annual average 826 of 41 ± 15.9 ppb. Similarly, Wang et al. (2009b) measured that air masses from eastern China had an 827 average O₃ concentration of 48 ppb at a background station in Hong Kong, highlighting the significant 828 impact of inter-regional transport on coastal regions. 829 Stratospheric-tropospheric exchange (STE) is a critical vertical transport process contributing to 830 background O₃ levels, particularly in high-altitude and northern regions of China. This process is most 831 active during spring, when stratospheric O3 is transported downward into the troposphere (Ding and 832 Wang, 2006; Lu et al., 2019; Xu et al., 2018). Wang et al. (2011) estimated that STE contributes 833 approximately 7 ppb to background O₃ concentrations in northern China during the spring season. 834 Observations at the Mt. Waliguan Station on the Tibetan Plateau further support the importance of STE; 835 Xu et al. (2018) reported that STE contributes 8-12 ppb to background O₃ concentrations during spring. 836 Lu et al. (2019) found that STE processes contribute as much as 20 ppb to background O₃ concentration 837 in western China during March and April, with an average contribution of 1.8-8.7 ppb across China from 838 March to October. In lower-latitude regions such as the Pearl River Delta, Shen et al. (2019) demonstrated





839 that vertical transport processes, including STE, predominantly influence background O3 levels during 840 spring and autumn. These findings underscore the critical role of altitude and latitude in modulating the 841 magnitude of STE contributions. 842 5.5 Comparative analysis of background ozone levels: insights from China and global perspectives 843 Figure 7 presents a comparative analysis of background O₃ concentrations in China and several other 844 global regions, with a particular focus on the United States, Canada, Europe, Japan, and South Korea. 845 On average, background O_3 concentrations in China (40.3 \pm 12.0 ppb) are slightly higher than those 846 observed in the United States (35.7 ± 14.0 ppb) (Chan and Vet, 2010; Dolwick et al., 2015; Emery et al., 847 2012; Fiore et al., 2003, 2002a; Hirsch et al., 1996; Parrish et al., 2009; Parrish and Ennis, 2019; Steiner 848 et al., 2010; Vingarzan, 2004; Yan et al., 2021; Zhang et al., 2011) and Europe $(34.2 \pm 10.3 \text{ ppb})$ (Auvray 849 and Bey, 2005; Brönnimann et al., 2000; Kalabokas et al., 2000; Naja et al., 2003; Parrish et al., 2009; 850 Scheel et al., 1997; Vecchi and Valli, 1998; Vingarzan, 2004; Wilson et al., 2012). This suggests that 851 although developed regions have made significant progress in controlling anthropogenic O₃ precursors, 852 background O₃ remains a major concern due to various regional factors such as higher emissions, 853 industrial activity, and specific atmospheric conditions (Huang et al., 2015). In contrast, background O₃ 854 levels in China are significantly higher than those observed in Canada (26.9 ± 7.4 ppb) (Chan and Vet, 855 2010; Vingarzan, 2004), which is likely due to Canada's lower industrial activity, less dense population, 856 and colder climate that limits the photochemical processes necessary for O₃ formation. 857 When comparing China to other East Asian regions, the background O₃ concentration is slightly 858 higher than in South Korea (38.8 ± 11.74 ppb) (Ghim and Chang, 2000; Kim et al., 2023; Lam and 859 Cheung, 2022; Lee and Park, 2022; Yeo and Kim, 2021), but marginally lower than in Japan (45.4 ± 23.2) 860 ppb) (Akimoto et al., 2015; Lam and Cheung, 2022; Sunwoo et al., 1994; Tsutsumi et al., 1994). Detailed 861 information on the data, including a breakdown of regional and temporal distributions, is provided Table 862 S4. Notably, East Asian regions, including China, South Korea, and Japan, typically exhibit background 863 O₃ levels that are 3-20 ppb higher than those observed in Europe, the United States, and Canada. This 864 regional disparity is attributable to a combination of factors, including the region's warm climate, high 865 solar radiation, and the presence of industrialized areas that emit large quantities of O₃ precursors. These

867

868

869

870

871

872

873

874

875

876

877

878

879

880

881

882

883

884

885

886

887

888

889

890

891

892

Xu et al., 2019).





factors collectively enhance photochemical O₃ (Lee et al., 2021; Li et al., 2016; Nagashima et al., 2010; Yamaji et al., 2006). Furthermore, complex regional airflow patterns, including transboundary transport and local atmospheric dynamics, promote the accumulation of background O3, especially in densely populated urban centers. These findings underscore the critical need for regional cooperation in addressing O₃ pollution in East Asia, where transboundary influences and shared atmospheric conditions complicate the management of background O₃ levels. A more granular regional comparison reveals notable differences in background O3 concentrations among various regions of both China and the United States. Specifically, the difference in background O₃ concentrations between Central and Western China (including NWC and SWC) reaches 10 ppb, while the discrepancy between the Eastern and Western United States is as high as 13 ppb. Western China and the Western United States exhibit higher background O3 levels. In particular, the Los Angeles area in the Western United States reports background O₃ levels as high as 62 ppb (Parrish and Ennis, 2019), a phenomenon attributed to the region's combination of intense ultraviolet radiation, low humidity, and favorable atmospheric conditions for O₃ formation. Similarly, the higher altitudes of Western China enhance its susceptibility to stratospheric transport, which contributes to elevated O₃ concentrations. The Western United States is similarly influenced by trans-Pacific atmospheric transport, further exacerbating O3 levels. In contrast to the significant regional differences observed in China and the United States, background O₃ concentrations in Canada and Europe exhibit relatively small variations, typically ranging from 4 to 7 ppb. The limited variation in Canada can be attributed to factors such as its low population density, minimal industrial activity, and expansive natural vegetation, all of which, coupled with its cold climate, limit O3 production. In Europe, the relatively smaller regional differences are likely as a result of effective transnational air quality management and stringent pollution control policies, which have successfully minimized disparities in O₃ concentrations across the continent. The relatively uniform air quality management frameworks in these regions have helped mitigate large-scale emissions and reduce regional discrepancies in background O₃ levels (Miranda et al., 2015; Næss, 2004; Rodrigues et al., 2021;





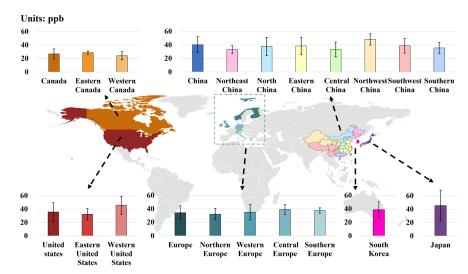


Figure 7: Average background O₃ concentrations in the United States, Canada, Europe, South Korea, Japan, and China.

6 Conclusions and perspectives

Background O_3 concentrations are critical for understanding O_3 pollution, as they represent the baseline level of O_3 even in the absence of local anthropogenic emissions. These concentrations determine the maximum achievable reduction in O_3 through the mitigation of anthropogenic precursor emissions, making accurate estimates crucial for effective air quality management and setting realistic pollution control targets. This study provides a comprehensive review of the definition and estimation methods for background O_3 concentrations, with a focus on recent advances in regional research in China. Our findings reveal an average background O_3 concentration of 40.3 ± 11.9 ppb in China, which accounts for 77 % of the tropospheric MDA8 O_3 . Notable spatial variations are observed, with the highest levels in Northwest China $(48.2 \pm 8.3 \text{ ppb})$ and the lowest in Northeast China $(33.0 \pm 5.7 \text{ ppb})$, alongside an upward national trend reflecting growing O_3 pollution. Despite progress in estimation methods, discrepancies persist across the four estimation methods, with the in situ measurement estimation method and statistical analysis estimation method yielding higher values, while the integrated method estimation method offers lower but more consistent estimates. Compared to other regions, East Asia, including China, South Korea, and Japan, experiences background O_3 levels 3-20 ppb higher than the United States,





Canada, and Europe. This highlights the region-specific atmospheric conditions and pollution characteristics, and the imperative of addressing background O₃ pollution within a global framework.

Although substantial progress has been made in estimating background O₃ over recent decades, considerable challenges remain due to the complexity of its sources and the multitude of influencing factors, particularly in the context of global climate changes and transboundary pollution. Future research should prioritize several key areas to advance the understanding and management of background O₃:

6.1 Accurate quantification of background ozone sources and processes

Natural emissions, long-range transport, and stratospheric-tropospheric exchange (STE) are key drivers of background O₃ concentrations; however, significant uncertainties remain in quantifying their individual contributions. To improve our understanding and predictive capabilities, future research must prioritize the refinement of quantification methods for these sources and processes. For instance, the variability of natural emissions, particularly from BVOCs and lightning, remains inadequately characterized across different climatic conditions. In addition, STE represents another critical but poorly understood source of background O₃, with studies indicating significant seasonal and regional variations in its contribution (Lu et al., 2019; Xie et al., 2017). Despite the critical importance of these processes, existing models often encounter difficulties in accurately simulating natural emissions and STE, primarily due to limitations in model structures and parameterization (Auvray and Bey, 2005; Griffiths et al., 2021; Huang et al., 2024; Koo et al., 2010). As a result, the accuracy of model predictions for background O₃ concentrations is compromised, resulting in increased uncertainties that hinder effective policy planning and air quality management.

6.2 Development of integrated method techniques

Single method approaches for estimating background O₃ concentrations have inherent limitations, as they often fail to capture the full spectrum of factors influencing O₃ levels. For example, while numerical models provide valuable insights, they frequently underestimate actual O₃ concentrations due to simplifications in chemical processes and uncertainties in input data. In contrast, statistical analysis estimation methods are heavily dependent on the availability and representativeness of observational

937

938

939

940

941

942

943

944

945

946

947

948

949

950

951

952

953

954

955

956

957

958

959

960

961

962

963





data, which can be sparse or biased, particularly in regions with limited monitoring networks. These limitations highlight the necessity for more integrated approaches that combine the strengths of different methods.

In this context, the development of integrated method techniques presents a promising approach to improve background O3 estimation. By integrating observational data, statistical analysis, and numerical results, integrated method estimation can mitigate the inherent limitations of each individual method. For example, data assimilation techniques, which combine model outputs with real-time observational data, have been shown to improve both spatial and temporal resolution, yielding more accurate and robust O₃ estimates (Skipper et al., 2021; Sun et al., 2024). Additionally, the integration of high-resolution regional models with long-term observational datasets can significantly enhance spatiotemporal coverage of background O₃ estimates, enabling precise characterization of O₃ variability across diverse geographic scales, from urban centers to remote rural areas. Recent advancements in machine learning-based fusion methods further extend the potential of data integration by uncovering nonlinear relationships among multiple data sources, thereby improving estimation accuracy. These approaches can also account for complex interactions between meteorological conditions, emission sources, and atmospheric chemistry, which are often challenging to capture using traditional methods. Given the potential of integrated method techniques to provide more accurate and comprehensive background O3 estimates, future research should prioritize their continued development and validation. Such efforts will improve the precision and reliability of background O₃ estimates, thereby enhancing our understanding of regional O₃ pollution dynamics and supporting the development of more effective air quality management strategies.

6.3 Fostering international collaboration on long-range pollution transport

As air quality standards for O₃ become increasingly stringent, background O₃ concentrations have emerged as a critical challenge for many countries in achieving regulatory targets. This issue is particularly pronounced in regions impacted by both local and transboundary pollution, where efforts to reduce domestic emissions may not fully address the underlying drivers of elevated background O₃ levels. For instance, studies conducted in the United States have demonstrated that despite substantial reductions

https://doi.org/10.5194/egusphere-2025-687 Preprint. Discussion started: 28 March 2025 © Author(s) 2025. CC BY 4.0 License.





in local emissions of O₃ precursors, background O₃ concentrations in some areas remain persistently high (Cooper et al., 2012; Huang et al., 2015). This phenomenon is partly attributed to long-range transport of pollutants, including O₃ precursors, from distant regions, often spanning international borders and even continents (Cynthia Lin et al., 2000; Dentener et al., 2010). Such transboundary pollution underscores the need for comprehensive international cooperation to effectively mitigate the challenges posed by background O₃.

International collaboration is therefore essential for tackling the elevated background O₃. To this end, fostering transboundary emission reduction agreements between countries and regions can play a pivotal role in curbing the long-range transport of O₃ and its precursors. Moreover, strengthening the global background O₃ monitoring network, particularly in remote regions and marine stations, would significantly enhance the capacity for real-time monitoring of background O₃ levels on a global scale.

6.4 Strengthening research on the interaction between background ozone and climate change

The impact of climate change on background O₃ concentrations represents a critical area for future research, with profound implications for air quality management and public health. Climate change is expected to affect background O₃ levels through multiple interconnected mechanisms. For example, rising temperatures and altered precipitation patterns are expected to affect natural emissions, such as BVOCs emissions from forests and NO_x emissions from soil, both of which are particularly sensitive to climatic factors like temperature and humidity. These changes would, in turn, influence regional background O₃ levels. Beyond these direct emission impacts, climate change is likely to modify atmospheric circulation patterns, thereby affecting the long-range transport of atmospheric pollutants and the spatial distribution of background O₃. Alterations in wind patterns and monsoon systems, for example, could significantly alter the transport of O₃ and its precursors over large distances, thereby exacerbating regional background O₃ levels, especially in areas downwind of major pollution sources (Collins et al., 2003; Sonwani et al., 2016; Sudo et al., 2003; Wu et al., 2008). Consequently, future research should prioritize understanding the dynamic interplay between climate change and background O₃ concentrations to improve predictive models and inform effective air quality management strategies.





991	Author contributions
992	CC collected the data.CC conducted the data analysis and prepared the draft with the support of WC, LG
993	and YW. XD, XW, and MS contributed to the revision of the paper.
994	
995	Competing interests
996	The authors declare that they have no conflict of interest.
997	
998	Acknowledgments
999	This study was supported by the National Key Research and Development Program of China
1000	(2023YFC3706205), the National Natural Science Foundation of China (42375109, 42121004), the
1001	Guangzhou Basic and Applied Basic Research Foundation (2024A04J0781), and the high-performance
1002	computing platform of Jinan University.
1002	n c
1003	References
1003	Akimoto, H., Mori, Y., Sasaki, K., Nakanishi, H., Ohizumi, T., and Itano, Y.: Analysis of monitoring data
1004	Akimoto, H., Mori, Y., Sasaki, K., Nakanishi, H., Ohizumi, T., and Itano, Y.: Analysis of monitoring data
1004 1005	Akimoto, H., Mori, Y., Sasaki, K., Nakanishi, H., Ohizumi, T., and Itano, Y.: Analysis of monitoring data of ground-level ozone in Japan for long-term trend during 1990-2010: Causes of temporal and spatial
1004 1005 1006	Akimoto, H., Mori, Y., Sasaki, K., Nakanishi, H., Ohizumi, T., and Itano, Y.: Analysis of monitoring data of ground-level ozone in Japan for long-term trend during 1990-2010: Causes of temporal and spatial variation, Atmos. Environ., 102, 302-310, https://doi.org/10.1016/j.atmosenv.2014.12.001, 2015.
1004 1005 1006 1007	Akimoto, H., Mori, Y., Sasaki, K., Nakanishi, H., Ohizumi, T., and Itano, Y.: Analysis of monitoring data of ground-level ozone in Japan for long-term trend during 1990-2010: Causes of temporal and spatial variation, Atmos. Environ., 102, 302-310, https://doi.org/10.1016/j.atmosenv.2014.12.001, 2015. Altshuller, A. P. and Lefohn, A. S.: Background ozone in the planetary boundary layer over the United
1004 1005 1006 1007 1008	Akimoto, H., Mori, Y., Sasaki, K., Nakanishi, H., Ohizumi, T., and Itano, Y.: Analysis of monitoring data of ground-level ozone in Japan for long-term trend during 1990-2010: Causes of temporal and spatial variation, Atmos. Environ., 102, 302-310, https://doi.org/10.1016/j.atmosenv.2014.12.001, 2015. Altshuller, A. P. and Lefohn, A. S.: Background ozone in the planetary boundary layer over the United States, J. Air Waste Manage., 46, 134-141, https://doi.org/10.1080/10473289.1996.10467445, 1996.
1004 1005 1006 1007 1008 1009	Akimoto, H., Mori, Y., Sasaki, K., Nakanishi, H., Ohizumi, T., and Itano, Y.: Analysis of monitoring data of ground-level ozone in Japan for long-term trend during 1990-2010: Causes of temporal and spatial variation, Atmos. Environ., 102, 302-310, https://doi.org/10.1016/j.atmosenv.2014.12.001, 2015. Altshuller, A. P. and Lefohn, A. S.: Background ozone in the planetary boundary layer over the United States, J. Air Waste Manage., 46, 134-141, https://doi.org/10.1080/10473289.1996.10467445, 1996. Auvray, M. and Bey, I.: Long-range transport to Europe: Seasonal variations and implications for the
1004 1005 1006 1007 1008 1009	Akimoto, H., Mori, Y., Sasaki, K., Nakanishi, H., Ohizumi, T., and Itano, Y.: Analysis of monitoring data of ground-level ozone in Japan for long-term trend during 1990-2010: Causes of temporal and spatial variation, Atmos. Environ., 102, 302-310, https://doi.org/10.1016/j.atmosenv.2014.12.001, 2015. Altshuller, A. P. and Lefohn, A. S.: Background ozone in the planetary boundary layer over the United States, J. Air Waste Manage., 46, 134-141, https://doi.org/10.1080/10473289.1996.10467445, 1996. Auvray, M. and Bey, I.: Long-range transport to Europe: Seasonal variations and implications for the European ozone budget, J. Geophys. ResAtmos., 110, 1-22, https://doi.org/10.1029/2004JD005503,
1004 1005 1006 1007 1008 1009 1010	Akimoto, H., Mori, Y., Sasaki, K., Nakanishi, H., Ohizumi, T., and Itano, Y.: Analysis of monitoring data of ground-level ozone in Japan for long-term trend during 1990-2010: Causes of temporal and spatial variation, Atmos. Environ., 102, 302-310, https://doi.org/10.1016/j.atmosenv.2014.12.001, 2015. Altshuller, A. P. and Lefohn, A. S.: Background ozone in the planetary boundary layer over the United States, J. Air Waste Manage., 46, 134-141, https://doi.org/10.1080/10473289.1996.10467445, 1996. Auvray, M. and Bey, I.: Long-range transport to Europe: Seasonal variations and implications for the European ozone budget, J. Geophys. ResAtmos., 110, 1-22, https://doi.org/10.1029/2004JD005503, 2005.
1004 1005 1006 1007 1008 1009 1010 1011 1012	Akimoto, H., Mori, Y., Sasaki, K., Nakanishi, H., Ohizumi, T., and Itano, Y.: Analysis of monitoring data of ground-level ozone in Japan for long-term trend during 1990-2010: Causes of temporal and spatial variation, Atmos. Environ., 102, 302-310, https://doi.org/10.1016/j.atmosenv.2014.12.001, 2015. Altshuller, A. P. and Lefohn, A. S.: Background ozone in the planetary boundary layer over the United States, J. Air Waste Manage., 46, 134-141, https://doi.org/10.1080/10473289.1996.10467445, 1996. Auvray, M. and Bey, I.: Long-range transport to Europe: Seasonal variations and implications for the European ozone budget, J. Geophys. ResAtmos., 110, 1-22, https://doi.org/10.1029/2004JD005503, 2005. Berlin, S. R., Langford, A. O., Estes, M., Dong, M., and Parrish, D. D.: Magnitude, decadal changes, and
1004 1005 1006 1007 1008 1009 1010 1011 1012 1013	Akimoto, H., Mori, Y., Sasaki, K., Nakanishi, H., Ohizumi, T., and Itano, Y.: Analysis of monitoring data of ground-level ozone in Japan for long-term trend during 1990-2010: Causes of temporal and spatial variation, Atmos. Environ., 102, 302-310, https://doi.org/10.1016/j.atmosenv.2014.12.001, 2015. Altshuller, A. P. and Lefohn, A. S.: Background ozone in the planetary boundary layer over the United States, J. Air Waste Manage., 46, 134-141, https://doi.org/10.1080/10473289.1996.10467445, 1996. Auvray, M. and Bey, I.: Long-range transport to Europe: Seasonal variations and implications for the European ozone budget, J. Geophys. ResAtmos., 110, 1-22, https://doi.org/10.1029/2004JD005503, 2005. Berlin, S. R., Langford, A. O., Estes, M., Dong, M., and Parrish, D. D.: Magnitude, decadal changes, and impact of regional background ozone transported into the Greater Houston, Texas, area, Environ. Sci.





1017 background ozone at different elevations in Switzerland (1992-1998), Atmos. Environ., 34, 5191-5198, 1018 https://doi.org/10.1016/S1352-2310(00)00193-X, 2000. 1019 Chan, C. Y., Chan, L. Y., and Harris, J. M.: Urban and background ozone trend in 1984-1999 at 1020 subtropical Hong Kong, South China, Ozone-Sci. 25, 513-522, Eng., 1021 https://doi.org/10.1080/01919510390481829, 2003. 1022 Chan, E. and Vet, R. J.: Baseline levels and trends of ground level ozone in Canada and the United States, 1023 Atmos. Chem. Phys., 10, 8629-8647, https://doi.org/10.5194/acp-10-8629-2010, 2010. 1024 Chen, J.: Spatial and temporal variation of ozone concentration and its influencing factors from 2017 to 1025 2020 in Northeast China, M.S. theses, Harbin Normal University, 40 pp., 2024. 1026 Chen, W., Guenther, A. B., Shao, M., Yuan, B., Jia, S., Mao, J., Yan, F., Krishnan, P., and Wang, X.: 1027 Assessment of background ozone concentrations in China and implications for using region-specific 1028 volatile organic compounds emission abatement to mitigate air pollution, Environ. Pollut., 305, 1029 119254, https://doi.org/10.1016/j.envpol.2022.119254, 2022. 1030 Chen, X.: Analysis of total ozone distribution and its influencing factors in western China based on 1031 satellite remote sensing, M.S. theses, Northwest Normal University, 55 pp., 2020. 1032 Cheng, Y., Wang, Y., Zhang, Y., Crawford, J. H., Diskin, G. S., Weinheimer, A. J., and Fried, A.: Estimator 1033 of surface ozone using formaldehyde and carbon monoxide concentrations over the eastern United 1034 States in summer, J. Geophys. Res.-Atmos., 123, 7642-7655, https://doi.org/10.1029/2018JD028452, 1035 2018. 1036 Collins, W. J., Derwent, R. G., Garnier, B., Johnson, C. E., Sanderson, M. G., and Stevenson, D. S.: 1037 Effect of stratosphere-troposphere exchange on the future tropospheric ozone trend, J. Geophys. Res.-1038 Atmos., 108, 1-10, https://doi.org/10.1029/2002JD002617, 2003. 1039 Cooper, O. R., Gao, R. S., Tarasick, D., Leblanc, T., and Sweeney, C.: Long-term ozone trends at rural 1040 ozone monitoring sites across the United States, 1990-2010, J. Geophys. Res.-Atmos., 117, 1-24, 1041 https://doi.org/10.1029/2012JD018261, 2012. 1042 Crutzen, P. J.: Photochemical reactions initiated by and influencing ozone in unpolluted tropospheric air, 1043 Tellus, 26, 47-57, https://doi.org/10.3402/tellusa.v26i1-2.9736, 1974.





1044 Cynthia Lin, C., Jacob, D. J., Munger, J. W., and Fiore, A. M.: Increasing background ozone in surface 1045 air over the United States, Geophys. Res. Lett., 27, 3465-3468, https://doi.org/10.1029/2000GL011762, 1046 2000. 1047 Dentener, F., Keating, T., and Akimoto, H. (Eds.): Hemispheric transport of air pollution 2010: Part A: 1048 Ozone and particulate matter, United Nations, New York and Geneva, 278 pp., ISBN 9789211170436, 1049 2010. 1050 Ding, A. and Wang, T.: Influence of stratosphere-to-troposphere exchange on the seasonal cycle of 1051 surface ozone at Mount Waliguan in western China, Geophys. Res. Lett., 33, 1-4, 1052 https://doi.org/10.1029/2005GL024760, 2006. 1053 Dolwick, P., Akhtar, F., Baker, K. R., Possiel, N., Simon, H., and Tonnesen, G.: Comparison of 1054 background ozone estimates over the western United States based on two separate model 1055 methodologies, Atmos. Environ., 109, 282-296, https://doi.org/10.1016/j.atmosenv.2015.01.005, 2015. 1056 Duc, H., Azzi, M., Wahid, H., and Ha, Q. P.: Background ozone level in the Sydney Basin: Assessment 1057 and trend analysis, Int. J. Climatol., 33, 2298-2308, https://doi.org/10.1002/joc.3595, 2013. 1058 Ehhalt, D., Prather, M., Dentener, F., Derwent, R., Dlugokencky, E., Holland, E., Isaksen, I., Katima, 1059 J., Kirchhoff, V., Matson, P., Midgley, P., and Wang, M.: Atmospheric chemistry and greenhouse 1060 gases, in: Climate Change 2001: The Scientific Basis. Contribution of Working Group I to the 1061 Third Assessment Report of the Intergovernmental Panel on Climate Change, edited by: 1062 Houghton, J. T., Ding, Y., Griggs, D. J., Noguer, M., van der Linder, P. J., Dai, X., Maskell, K., 1063 and Johnson, C. A., Cambridge University Press, Cambridge, UK, New York, NY, USA, 239-287, 1064 2001. 1065 Emery, C., Jung, J., Downey, N., Johnson, J., Jimenez, M., Yarwood, G., and Morris, R.: Regional and 1066 global modeling estimates of Policy Relevant Background ozone over the United States, Atmos. 1067 Environ., 47, 206-217, https://doi.org/10.1016/j.atmosenv.2011.11.012, 2012. 1068 Fiore, A., Jacob, D. J., Liu, H., Yantosca, R. M., Fairlie, T. D., and Li, Q.: Variability in surface ozone 1069 background over the United States: Implications for air quality policy, J. Geophys. Res.-Atmos., 108, 1070 1-19, https://doi.org/10.1029/2003JD003855, 2003.





1071 Fiore, A. M., Jacob, D. J., Bey, I., Yantosca, R. M., Field, B. D., Fusco, A. C., and Wilkinson, J. G.: 1072 Background ozone over the United States in summer: Origin, trend, and contribution to pollution 1073 episodes, J. Geophys. Res.-Atmos., 107, 1-25, https://doi.org/10.1029/2001JD000982, 2002a. 1074 Fiore, A. M., Jacob, D. J., Field, B. D., Streets, D. G., Fernandes, S. D., and Jang, C.: Linking ozone 1075 pollution and climate change: The case for controlling methane, Geophys. Res. Lett., 29, 25-1-25-4, 1076 https://doi.org/10.1029/2002GL015601, 2002b. 1077 Fiore, A. M., Oberman, J. T., Lin, M. Y., Zhang, L., Clifton, O. E., Jacob, D. J., Naik, V., Horowitz, L. 1078 W., Pinto, J. P., and Milly, G. P.: Estimating North American background ozone in U.S. surface air 1079 with two independent global models: Variability, uncertainties, and recommendations, Atmos. 1080 Environ., 96, 284-300, https://doi.org/10.1016/j.atmosenv.2014.07.045, 2014. 1081 Galbally, I. E., Miller, A. J., Hoy, R. D., Ahmet, S., Joynt, R. C., and Attwood, D.: Surface ozone at rural 1082 sites in the Latrobe Valley and Cape Grim, Australia, Atmos. Environ. (1967), 20, 2403-2422, 1083 https://doi.org/10.1016/0004-6981(86)90071-5, 1986. 1084 Gao, J., Wang, T., Ding, A., and Liu, C.: Observational study of ozone and carbon monoxide at the 1085 summit of Mount Tai (1534m a.s.l.) in central-eastern China, Atmos. Environ., 39, 4779-4791, 1086 https://doi.org/10.1016/j.atmosenv.2005.04.030, 2005. 1087 Geng, G., Liu, Y., Liu, Y., Liu, S., Cheng, J., Yan, L., Wu, N., Hu, H., Tong, D., Zheng, B., Yin, Z., He, 1088 K., and Zhang, Q.: Efficacy of China's clean air actions to tackle PM2.5 pollution between 2013 and 1089 2020, Nat. Geosci., 17, 987-994, https://doi.org/10.1038/s41561-024-01540-z, 2024. 1090 Ghim, Y. S. and Chang, Y.: Characteristics of ground-level ozone distributions in Korea for the period of 1091 1990-1995, J. Geophys. Res.-Atmos., 105, 8877-8890, https://doi.org/10.1029/1999JD901179, 2000. 1092 Govender, P. and Sivakumar, V.: Application of k-means and hierarchical clustering techniques for 1093 analysis of air pollution: A review (1980-2019), Atmos. Pollut. Res., 11, 40-56, https://doi.org/10.1016/j.apr.2019.09.009, 2020. 1094 1095 Griffiths, P. T., Murray, L. T., Zeng, G., Shin, Y. M., Abraham, N. L., Archibald, A. T., Deushi, M., 1096 Emmons, L. K., Galbally, I. E., Hassler, B., Horowitz, L. W., Keeble, J., Liu, J., Moeini, O., Naik, V., 1097 O'Connor, F. M., Oshima, N., Tarasick, D., Tilmes, S., Turnock, S. T., Wild, O., Young, P. J., and Zanis,





1098 P.: Tropospheric ozone in CMIP6 simulations, Atmos. Chem. Phys., 21, 4187-4218, 1099 https://doi.org/10.5194/acp-21-4187-2021, 2021. 1100 Guo, J. J., Fiore, A. M., Murray, L. T., Jaffe, D. A., Schnell, J. L., Moore, C. T., and Milly, G. P.: Average 1101 versus high surface ozone levels over the continental USA: Model bias, background influences, and 1102 interannual variability, Atmos. Chem. Phys., 18, 12123-12140, https://doi.org/10.5194/acp-18-12123-1103 2018, 2018. 1104 Haagen-Smit, A. J.: Chemistry and physiology of Los Angeles Smog, Ind. Eng. Chem., 44, 1342-1346, 1105 https://doi.org/10.1021/ie50510a045, 1952. 1106 He, C., Mu, H., Yang, L., Wang, D., Di, Y., Ye, Z., Yi, J., Ke, B., Tian, Y., and Hong, S.: Spatial variation 1107 of surface ozone concentration during the warm season and its meteorological driving factors in China, 1108 Environm. Sci., 42, 4168-4179, https://doi.org/10.13227/j.hjkx.202009228, 2021. 1109 He, C., Wu, Q., Li, B., Liu, J., Gong, X., and Zhang, L.: Surface ozone pollution in China: Trends, 1110 Public Health, 11, 1131753, exposure risks, and drivers, Front. 1111 https://doi.org/10.3389/fpubh.2023.1131753, 2023. 1112 Hirsch, A. I., Munger, J. W., Jacob, D. J., Horowitz, L.W., and Goldstein, A. H.: Seasonal variation of 1113 the ozone production efficiency per unit NOx at Harvard Forest, Massachusetts, J. Geophys. Res.-1114 Atmos., 101, 12659-12666, 1996. 1115 Hogrefe, C., Liu, P., Pouliot, G., Mathur, R., Roselle, S., Flemming, J., Lin, M., and Park, R. J.: Impacts 1116 of different characterizations of large-scale background on simulated regional-scale ozone over the 1117 continental United States, Atmos. Chem. Phys., 18, 3839-3864, https://doi.org/10.5194/acp-18-3839-1118 2018, 2018. 1119 Hosseinpour, F., Kumar, N., Tran, T., and Knipping, E.: Using machine learning to improve the estimate 1120 U.S. background Environ., 316, 120145, ozone, Atmos. 1121 https://doi.org/10.1016/j.atmosenv.2023.120145, 2024. 1122 Hu, C., Kang, P., Wu, K., Zhang, X., Wang, S., Wang, Z., Ouyang, Z., Zeng, S., and Wei, X.: Study of 1123 the spatial and temporal distribution of ozone and its influence factors over Sichuan Basin based on 1124 generalized additive model, Scien. Circum., 39, 809-820, Acta





- $1125 \hspace{1.5cm} https://doi.org/10.13671/j.hjkxxb.2018.0444, 2019. \\$
- $1126 \qquad \text{Huang, L., Zhao, X., Chen, C., Tan, J., Li, Y., Chen, H., Wang, Y., Li, L., Guenther, A., and Huang, H.:} \\$
- 1127 Uncertainties of biogenic VOC emissions caused by land cover data and implications on ozone
- 1128 mitigation strategies for the Yangtze River Delta region, Atmos. Environ., 337, 120765,
- 1129 https://doi.org/10.1016/j.atmosenv.2024.120765, 2024.
- Huang, M., Bowman, K. W., Carmichael, G. R., Lee, M., Chai, T., Spak, S. N., Henze, D. K., Darmenov,
- 1131 A. S., and da Silva, A. M.: Improved western U.S. background ozone estimates via constraining
- nonlocal and local source contributions using Aura TES and OMI observations, J. Geophys. Res.-
- 1133 Atmos., 120, 3572-3592, https://doi.org/10.1002/2014JD022993, 2015.
- 1134 Itano, Y., Bandow, H., Takenaka, N., Saitoh, Y., Asayama, A., and Fukuyama, J.: Impact of NO_x reduction
- on long-term ozone trends in an urban atmosphere, Sci. Total Environ., 379, 46-55,
- 1136 https://doi.org/10.1016/j.scitotenv.2007.01.079, 2007.
- Jackson, R. B., Saunois, M., Martinez, A., Canadell, J. G., Yu, X., Li, M., Poulter, B., Raymond, P. A.,
- 1138 Regnier, P., Ciais, P., Davis, S. J., and Patra, P. K.: Human activities now fuel two-thirds of global
- methane emissions, Environ. Res. Lett., 19, 101002, https://doi.org/10.1088/1748-9326/ad6463, 2024.
- 1140 Jacob, D. J., Logan, J. A., and Murti, P. P.: Effect of rising Asian emissions on surface ozone in the United
- States, Geophys. Res. Lett., 26, 2175-2178, https://doi.org/10.1029/1999GL900450, 1999.
- Jaffe, D. A., Cooper, O. R., Fiore, A. M., Henderson, B. H., Tonnesen, G. S., Russell, A. G., Henze, D.
- 1143 K., Langford, A. O., Lin, M., and Moore, T.: Scientific assessment of background ozone over the U.S.:
- 1144 Implications for air quality management, Elementa-Sci. Anthrop., 6, 56,
- 1145 https://doi.org/10.1525/elementa.309, 2018.
- 1146 Jenkin, M. E.: Trends in ozone concentration distributions in the UK since 1990: Local, regional and
- global influences, Atmos. Environ., 42, 5434-5445, https://doi.org/10.1016/j.atmosenv.2008.02.036,
- 1148 2008.
- Jolliffe, I.: Principal Component Analysis, in: Encyclopedia of statistics in behavioral science, edited by:
- Everitt, B. S. and Howell, D. C., John Wiley and Sons, Ltd., Chichester, 1580-1584,
- 1151 https://doi.org/10.1002/0470013192.bsa501, 2005.





1152 Kalabokas, P. D., Viras, L. G., Bartzis, J. G., and Repapis, C. C.: Mediterranean rural ozone 1153 characteristics around the urban area of Athens, Atmos. Environ., 34, 5199-5208, 1154 https://doi.org/10.1016/S1352-2310(00)00298-3, 2000. 1155 Kashinath, K., Mustafa, M., Albert, A., Wu, J., Jiang, C., Esmaeilzadeh, S., Azizzadenesheli, K., Wang, 1156 R., Chattopadhyay, A., Singh, A., Manepalli, A., Chirila, D., Yu, R., Walters, R., White, B., Xiao, H., 1157 Tchelepi, H. A., Marcus, P., Anandkumar, A., Hassanzadeh, P., and Prabhat: Physics-informed machine 1158 learning: Case studies for weather and climate modelling, Philos. T. R. Soc. A., 379, 20200093, 1159 https://doi.org/10.1098/rsta.2020.0093, 2021. 1160 Kemball-Cook, S., Parrish, D., Ryerson, T., Nopmongcol, U., Johnson, J., Tai, E., and Yarwood, G.: 1161 Contributions of regional transport and local sources to ozone exceedances in Houston and Dallas: 1162 Comparison of results from a photochemical grid model to aircraft and surface measurements, J. 1163 Geophys. Res.-Atmos., 114, 1-14, https://doi.org/10.1029/2008JD010248, 2009. 1164 Kim, S., Kim, K., Jeong, Y., Seo, S., Park, Y., and Kim, J.: Changes in surface ozone in South Korea on 1165 diurnal to decadal timescales for the period of 2001-2021, Atmos. Chem. Phys., 23, 12867-12886, 1166 https://doi.org/10.5194/acp-23-12867-2023, 2023. 1167 Kirschke, S., Bousquet, P., Ciais, P., Saunois, M., Canadell, J. G., Dlugokencky, E. J., Bergamaschi, P., 1168 Bergmann, D., Blake, D. R., Bruhwiler, L., Cameron-Smith, P., Castaldi, S., Chevallier, F., Feng, L., 1169 Fraser, A., Heimann, M., Hodson, E. L., Houweling, S., Josse, B., Fraser, P. J., Krummel, P. B., 1170 Lamarque, J. F., Langenfelds, R. L., Le Quere, C., Naik, V., O'Doherty, S., Palmer, P. I., Pison, I., 1171 Plummer, D., Poulter, B., Prinn, R. G., Rigby, M., Ringeval, B., Santini, M., Schmidt, M., Shindell, D. 1172 T., Simpson, I. J., Spahni, R., Steele, L. P., Strode, S. A., Sudo, K., Szopa, S., van der Werf, G. R., 1173 Voulgarakis, A., van Weele, M., Weiss, R. F., Williams, J. E., and Zeng, G.: Three decades of global 1174 methane sources and sinks, Nat. Geosci., 6, 813-823, https://doi.org/10.1038/ngeo1955, 2013. 1175 Koo, B., Chien, C., Tonnesen, G., Morris, R., Johnson, J., Sakulyanontvittaya, T., Piyachaturawat, P., and 1176 Yarwood, G.: Natural emissions for regional modeling of background ozone and particulate matter 1177 and impacts on emissions control strategies, Atmos. Environ., 44, 2372-2382, 1178 https://doi.org/10.1016/j.atmosenv.2010.02.041, 2010.





- 1179 Lam, Y. F. and Cheung, H. M.: Investigation of Policy Relevant Background (PRB) ozone in East Asia,
- Atmosphere-Basel, 13, 723, https://doi.org/10.3390/atmos13050723, 2022.
- Langford, A. O., Senff, C. J., Banta, R. M., Hardesty, R. M., Alvarez II, R. J., Sandberg, S. P., and Darby,
- 1182 L. S.: Regional and local background ozone in Houston during Texas Air Quality Study 2006, J.
- 1183 Geophys. Res.-Atmos., 114, 1-12, https://doi.org/10.1029/2008JD011687, 2009.
- 1184 Lassey, K. R., Lowe, D. C., and Manning, M. R.: The trend in atmospheric methane δ13C and
- implications for isotopic constraints on the global methane budget, Global Biogeochem. Cy., 14, 41-
- 49, https://doi.org/10.1029/1999GB900094, 2000.
- 1187 Lee, H., Chang, L., Jaffe, D. A., Bak, J., Liu, X., Abad, G. G., Jo, H., Jo, Y., Lee, J., and Kim, C.: Ozone
- 1188 continues to increase in East Asia despite decreasing NO₂: Causes and abatements, Remote Sens.-
- 1189 Basel, 13, 2177, https://doi.org/10.3390/rs13112177, 2021.
- 1190 Lee, H. and Park, R. J.: Factors determining the seasonal variation of ozone air quality in South Korea:
- 1191 Regional background versus domestic emission contributions, Environ. Pollut., 308, 119645,
- https://doi.org/10.1016/j.envpol.2022.119645, 2022.
- 1193 Lefohn, A. S., Emery, C., Shadwick, D., Wernli, H., Jung, J., and Oltmans, S. J.: Estimates of background
- surface ozone concentrations in the United States based on model-derived source apportionment,
- Atmos. Environ., 84, 275-288, https://doi.org/10.1016/j.atmosenv.2013.11.033, 2014.
- 1196 Lelieveld, J., Crutzen, P. J., and Dentener, F. J.: Changing concentration, lifetime and climate forcing of
- atmospheric methane, Tellus B, 50, 128-150, https://doi.org/10.1034/j.1600-0889.1998.t01-1-00002.x,
- 1198 1998.
- 1199 Li, J., Yang, W., Wang, Z., Chen, H., Hu, B., Li, J., Sun, Y., Fu, P., and Zhang, Y.: Modeling study of
- surface ozone source-receptor relationships in East Asia, Atmos. Res., 167, 77-88,
- 1201 https://doi.org/10.1016/j.atmosres.2015.07.010, 2016.
- 1202 Li, K., Jacob, D. J., Liao, H., Shen, L., Zhang, Q., and Bates, K. H.: Anthropogenic drivers of 2013-2017
- 1203 trends in summer surface ozone in China, P. Natl. A. Sci. U.S.A., 116, 422-427,
- 1204 https://doi.org/10.1073/pnas.1812168116, 2019.
- 1205 Li, K., Jacob, D. J., Shen, L., Lu, X., De Smedt, I., and Liao, H.: Increases in surface ozone pollution in





- 1206 China from 2013 to 2019: Anthropogenic and meteorological influences, Atmos. Chem. Phys., 20,
- 1207 11423-11433, https://doi.org/10.5194/acp-20-11423-2020, 2020.
- 1208 Li, N., He, Q., Greenberg, J., Guenther, A., Li, J., Cao, J., Wang, J., Liao, H., Wang, Q., and Zhang, Q.:
- 1209 Impacts of biogenic and anthropogenic emissions on summertime ozone formation in the Guanzhong
- 1210 Basin, China, Atmos. Chem. Phys., 18, 7489-7507, https://doi.org/10.5194/acp-18-7489-2018, 2018.
- 1211 Li, X., Liu, J., Mauzerall, D. L., Emmons, L. K., Walters, S., Horowitz, L. W., and Tao, S.: Effects of
- 1212 trans-Eurasian transport of air pollutants on surface ozone concentrations over western China, J.
- 1213 Geophys. Res.-Atmos., 119, 12338-12354, https://doi.org/10.1002/2014JD021936, 2014.
- 1214 Li, Y., Lau, A. K., Fung, J. C., Zheng, J. Y., Zhong, L. J., and Louie, P. K. K.: Ozone source apportionment
- 1215 (OSAT) to differentiate local regional and super-regional source contributions in the Pearl River Delta
- 1216 region, China, J. Geophys. Res.-Atmos., 117, 1-18, https://doi.org/10.1029/2011JD017340, 2012.
- 1217 Liang, Y., Liu, Y., Wang, H., Li, L., Duan, Y., and Lu, K.: Regional characteristics of ground-level ozone
- 1218 in Shanghai based on PCA analysis, Acta Scien. Circum., 38, 3807-3815,
- 1219 https://doi.org/10.13671/j.hjkxxb.2018.0209, 2018.
- 1220 Liao, W., Wu, L., Zhou, S., Wang, X., and Chen, D.: Impact of synoptic weather types on ground-level
- 1221 ozone concentrations in Guangzhou, China, Asia-Pac. J. Atmos. Sci., 57, 169-180,
- 1222 https://doi.org/10.1007/s13143-020-00186-2, 2021.
- 1223 Liu, N., Lin, W., Ma, J., Xu, W., and Xu, X.: Seasonal variation in surface ozone and its regional
- 1224 characteristics at global atmosphere watch stations in China, J. Environ. Sci., 77, 291-302,
- 1225 https://doi.org/10.1016/j.jes.2018.08.009, 2019.
- 1226 Liu, N., Li, X., Ren, W., and Wan, R.: Influence of East Asian summer monsoon on ozone transport in
- 1227 eastern China, Trans. Atmos. Sci. (in Chinese), 44, 261-269,
- 1228 https://doi.org/10.13878/j.cnki.dqkxxb.20200706001, 2021.
- 1229 Liu, S. C., Trainer, M., Fehsenfeld, F. C., Parrish, D. D., Williams, E. J., Fahey, D. W., Hübler, G., and
- Murphy, P. C.: Ozone production in the rural troposphere and the implications for regional and global
- 1231 ozone distributions, J. Geophys. Res.-Atmos., 92, 4191-4207,
- 1232 https://doi.org/10.1029/JD092iD04p04191, 1987.





- 1233 Lu, X., Zhang, L., Chen, Y., Zhou, M., Zheng, B., Li, K., Liu, Y., Lin, J., Fu, T., and Zhang, Q.: Exploring
- 1234 2016-2017 surface ozone pollution over China: Source contributions and meteorological influences,
- 1235 Atmos. Chem. Phys., 19, 8339-8361, https://doi.org/10.5194/acp-19-8339-2019, 2019.
- 1236 Ma, J., Zheng, X., and Xu, X.: Comment on "Why does surface ozone peak in summertime at Waliguan?"
- 1237 by Bin Zhu et al., Geophys. Res. Lett., 32, 1-2, https://doi.org/10.1029/2004GL021683, 2005.
- 1238 Ma, Z., Xu, J., Quan, W., Zhang, Z., Lin, W., and Xu, X.: Significant increase of surface ozone at a rural
- site, north of eastern China, Atmos. Chem. Phys., 16, 3969-3977, https://doi.org/10.5194/acp-16-
- 1240 3969-2016, 2016.
- 1241 Mahmud, A., Tyree, M., Cayan, D., Motallebi, N., and Kleeman, M. J.: Statistical downscaling of climate
- 1242 change impacts on ozone concentrations in California, J. Geophys. Res.-Atmos., 113, 1-12,
- 1243 https://doi.org/10.1029/2007JD009534, 2008.
- 1244 McDonald-Buller, E. C., Allen, D. T., Brown, N., Jacob, D. J., Jaffe, D., Kolb, C. E., Lefohn, A. S.,
- 1245 Oltmans, S., Parrish, D. D., Yarwood, G., and Zhang, L.: Establishing Policy Relevant Background
- 1246 (PRB) ozone concentrations in the United States, Environ. Sci. Technol., 45, 9484-9497,
- 1247 https://doi.org/10.1021/es2022818, 2011.
- 1248 Miranda, A., Silveira, C., Ferreira, J., Monteiro, A., Lopes, D., Relvas, H., Borrego, C., and Roebeling,
- P.: Current air quality plans in Europe designed to support air quality management policies, Atmos.
- Pollut. Res., 6, 434-443, https://doi.org/10.5094/APR.2015.048, 2015.
- 1251 Næss, T.: The Effectiveness of the EU's ozone policy, Int. Environ. Agreem.-P, 4, 47-63,
- 1252 https://doi.org/10.1023/B:INEA.0000019051.06627.2e, 2004.
- 1253 Nagashima, T., Ohara, T., Sudo, K., and Akimoto, H.: The relative importance of various source regions
- 1254 on East Asian surface ozone, Atmos. Chem. Phys., 10, 11305-11322, https://doi.org/10.5194/acp-10-
- 1255 11305-2010, 2010.
- 1256 Naja, M., Akimoto, H., and Staehelin, J.: Ozone in background and photochemically aged air over central
- 1257 Europe: Analysis of long-term ozonesonde data from Hohenpeissenberg and Payerne, J. Geophys.
- 1258 Res.-Atmos., 108, 1-11, https://doi.org/10.1029/2002JD002477, 2003.
- 1259 Ni, R., Lin, J., Yan, Y., and Lin, W.: Foreign and domestic contributions to springtime ozone over China,





1260 Atmos. Chem. Phys., 18, 11447-11469, https://doi.org/10.5194/acp-18-11447-2018, 2018. 1261 Nie, H., Niu, S., Wang, Z., Tang, J., and Zhao, Y.: Characteristic analysis of surface ozone over clean 1262 area in Qinghai-Xizang Plateau, Journal of Arid Meteorology, 22, 1-7, 2004. 1263 Nielsen-Gammon, J. W., Tobin, J., McNeel, A., and Li, G.: A conceptual model for eight-hour ozone 1264 exceedances in Houston, Texas Part I: Background ozone levels in eastern Texas, Center for 1265 Atmospheric Chemistry and the Environment, Texas A&M University, Open File Rep., 52 pp., 2005. 1266 Ning, Z., Gao, S., Gu, Z., Ni, C., Fang, F., Nie, Y., Jiao, Z., and Wang, C.: Prediction and explanation for 1267 ozone variability using cross-stacked ensemble learning model, Sci. Total Environ., 935, 173382, 1268 https://doi.org/10.1016/j.scitotenv.2024.173382, 2024. 1269 Nopmongcol, U., Jung, J., Kumar, N., and Yarwood, G.: Changes in US background ozone due to global 1270 anthropogenic emissions from 1970 to 2020, Atmos. Environ., 140. 446-455. 1271 https://doi.org/10.1016/j.atmosenv.2016.06.026, 2016. 1272 Ou-Yang, C., Hsieh, H., Wang, S., Lin, N., Lee, C., Sheu, G., and Wang, J.: Influence of Asian continental 1273 outflow on the regional background ozone level in northern South China Sea, Atmos. Environ., 78, 1274 144-153, https://doi.org/10.1016/j.atmosenv.2012.07.040, 2013. 1275 Ozone Pollution Control Committee of Chinese Society of Environmental Sciences: China blue book on 1276 prevention and control of atmospheric ozone pollution (2020), Science Press, Chinese mainland, 121 1277 pp., ISBN 9787030716644, 2022. 1278 Ozone Pollution Control Committee of Chinese Society of Environmental Sciences: China blue book on 1279 prevention and control of atmospheric ozone pollution (2023), Science Press, Chinese mainland, 164 1280 pp., ISBN 9787030781840, 2024. 1281 Parrish, D. D. and Ennis, C. A.: Estimating background contributions and US anthropogenic 1282 enhancements to maximum ozone concentrations in the northern US, Atmos. Chem. Phys., 19, 12587-1283 12605, https://doi.org/10.5194/acp-19-12587-2019, 2019. 1284 Parrish, D. D., Millet, D. B., and Goldstein, A. H.: Increasing ozone in marine boundary layer inflow at 1285 the west coasts of North America and Europe, Atmos. Chem. Phys., 9, 1303-1323, 1286 https://doi.org/10.5194/acp-9-1303-2009, 2009.





1287 Pfister, G. G., Walters, S., Emmons, L. K., Edwards, D. P., and Avise, J.: Quantifying the contribution of 1288 inflow on surface ozone over California during summer 2008, J. Geophys. Res.-Atmos., 118, 12282-1289 12299, https://doi.org/10.1002/2013JD020336, 2013. 1290 Prather, M. J., Holmes, C. D., and Hsu, J.: Reactive greenhouse gas scenarios: Systematic exploration of 1291 uncertainties and the role of atmospheric chemistry, Geophys. Res. Lett., 39, L09803, 1292 https://doi.org/10.1029/2012gl051440, 2012. 1293 Qin, L., Han, X., Zhang, M., and Liu, J.: Numerical simulation analysis on ozone source apportionment 1294 in the Yinchuan metropolitan area in summer, Climatic Environ. Res. (in Chinese), 28, 183-194, 1295 https://doi.org/10.3878/j.issn.1006-9585.2022.21186, 2023. 1296 Qin, Y., Liu, M., Song, J., Yu, R., Li, L., and Su, G.: Temporal and spatial variation characteristics of O₃ 1297 concentration in the surface layer over Guangdong-Hong Kong-Macao Greater Bay Area, China, Acta 1298 Scien. Circum., 41, 2987-3000, https://doi.org/10.13671/j.hjkxxb.2021.0065, 2021. 1299 Reid, N., Yap, D., and Bloxam, R.: The potential role of background ozone on current and emerging air 1300 issues: An overview, Air Qual. Atmos. Hlth., 1, 19-29, https://doi.org/10.1007/s11869-008-0005-z, 1301 2008. 1302 Riley, M. L., Jiang, N., Duc, H. N., and Azzi, M.: Long-term trends in inferred continental background 1303 ozone in eastern Australia, Atmosphere-Basel, 14, 1104, https://doi.org/10.3390/atmos14071104, 2023. 1304 Rizos, K., Meleti, C., Kouvarakis, G., Mihalopoulos, N., and Melas, D.: Determination of the background 1305 pollution in the eastern Mediterranean applying a statistical clustering technique, Atmos. Environ., 1306 276, 119067, https://doi.org/10.1016/j.atmosenv.2022.119067, 2022. 1307 Rodrigues, V., Gama, C., Ascenso, A., Oliveira, K., Coelho, S., Monteiro, A., Hayes, E., and Lopes, M.: 1308 Assessing air pollution in European cities to support a citizen centered approach to air quality 1309 management, Sci. Total Environ., 799, 149311, https://doi.org/10.1016/j.scitotenv.2021.149311, 2021. 1310 Sahu, S. K., Liu, S., Liu, S., Ding, D., and Xing, J.: Ozone pollution in China: Background and 1311 transboundary contributions to ozone concentration & related health effects across the country, Sci. 1312 Total Environ., 761, 144131, https://doi.org/10.1016/j.scitotenv.2020.144131, 2021. 1313 Saunois, M., Bousquet, P., Poulter, B., Peregon, A., Ciais, P., Canadell, J. G., Dlugokencky, E. J., Etiope,





1314 G., Bastviken, D., Houweling, S., Janssens-Maenhout, G., Tubiello, F. N., Castaldi, S., Jackson, R. B., 1315 Alexe, M., Arora, V. K., Beerling, D. J., Bergamaschi, P., Blake, D. R., Brailsford, G., Brovkin, V., 1316 Bruhwiler, L., Crevoisier, C., Crill, P., Covey, K., Curry, C., Frankenberg, C., Gedney, N., Höglund-1317 Isaksson, L., Ishizawa, M., Ito, A., Joos, F., Kim, H.-S., Kleinen, T., Krummel, P., Lamarque, J.-F., 1318 Langenfelds, R., Locatelli, R., Machida, T., Maksyutov, S., McDonald, K. C., Marshall, J., Melton, J. 1319 R., Morino, I., Naik, V., O'Doherty, S., Parmentier, F.-J. W., Patra, P. K., Peng, C., Peng, S., Peters, G. 1320 P., Pison, I., Prigent, C., Prinn, R., Ramonet, M., Riley, W. J., Saito, M., Santini, M., Schroeder, R., 1321 Simpson, I. J., Spahni, R., Steele, P., Takizawa, A., Thornton, B. F., Tian, H., Tohjima, Y., Viovy, N., 1322 Voulgarakis, A., van Weele, M., van der Werf, G. R., Weiss, R., Wiedinmyer, C., Wilton, D. J., 1323 Wiltshire, A., Worthy, D., Wunch, D., Xu, X., Yoshida, Y., Zhang, B., Zhang, Z., and Zhu, Q.: The 1324 global methane budget 2000-2012, Earth Syst. Sci. Data, 8, 697-751, https://doi.org/10.5194/essd-8-1325 697-2016, 2016. 1326 Scheel, H. E., Areskoug, H., Geiss, H., Gomiscek, B., Granby, K., Haszpra, L., Klasinc, L., Kley, D., 1327 Laurila, T., Lindskog, A., Roemer, M., Schmitt, R., Simmonds, P., Solberg, S., and Toupance, G.: On 1328 the spatial distribution and seasonal variation of lower-troposphere ozone over Europe, J. Atmos. 1329 Chem., 28, 11-28, https://doi.org/10.1023/A:1005882922435, 1997. 1330 Shen, J., He, L., Cheng, P., Xie, M., Jiang, M., Chen, D., and Zhou, G.: Characteristics of ozone 1331 concentration variation in the northern background site of the Pearl River Delta, Ecology and 1332 Environmental Sciences, 28, 2006-2011, https://doi.org/10.16258/j.cnki.1674-5906.2019.10.010, 1333 2019. 1334 Shen, L. and Wang, Y.: Changes in tropospheric ozone levels over the three representative regions of 1335 China observed from space by the Tropospheric Emission Spectrometer (TES), 2005-2010, Chinese 1336 Sci. Bull., 57, 2865-2871, https://doi.org/10.1007/s11434-012-5099-x, 2012. 1337 Shin, H. J., Cho, K. M., Han, J. S., Kim, J. S., and Kim, Y. P.: The effects of precursor emission and 1338 background concentration changes on the surface ozone concentration over Korea, Aerosol Air Qual. 1339 Res., 12, 93-103, https://doi.org/10.4209/aaqr.2011.09.0141, 2012. 1340 Sillman, S. and Samson, P. J.: Impact of temperature on oxidant photochemistry in urban, polluted rural





1341 and remote environments, Geophys. Res.-Atmos., 100, 11497-11508, 1342 https://doi.org/10.1029/94JD02146, 1995. 1343 Skipper, T. N., Hu, Y., Odman, M. T., Henderson, B. H., Hogrefe, C., Mathur, R., and Russell, A. G.: 1344 Estimating US background ozone using data fusion, Environ. Sci. Technol., 55, 4504-4512, 1345 https://doi.org/10.1021/acs.est.0c08625, 2021. 1346 Sonwani, S., Saxena, P., and Kulshrestha, U.: Role of global warming and plant signaling in BVOC 1347 emissions, in: Plant responses to air pollution, edited by: Kulshrestha, U. and Saxena, P., Springer, 1348 Singapore, 45-57, https://doi.org/10.1007/978-981-10-1201-3_5, 2016. 1349 Steiner, A. L., Davis, A. J., Sillman, S., Owen, R. C., Michalak, A. M., and Fiore, A. M.: Observed 1350 suppression of ozone formation at extremely high temperatures due to chemical and biophysical 1351 feedbacks, P. Natl. A. Sci. U.S.A., 107, 19685-19690, https://doi.org/10.1073/pnas.1008336107, 2010. 1352 Su, B.: Characteristics and impact factors of O₃ concentrations in mountain background region of East 1353 China, Environm. Sci., 34, 2519-2525, https://doi.org/10.13227/j.hjkx.2013.07.023, 2013. 1354 Suciu, L. G., Griffin, R. J., and Masiello, C. A.: Regional background O3 and NOx in the Houston-1355 Galveston-Brazoria (TX) region: A decadal-scale perspective, Atmos. Chem. Phys., 17, 6565-6581, 1356 https://doi.org/10.5194/acp-17-6565-2017, 2017. 1357 Sudo, K., Takahashi, M., and Akimoto, H.: Future changes in stratosphere-troposphere exchange and 1358 their impacts on future tropospheric ozone simulations, Geophys. Res. Lett., 30, 1-4, 1359 https://doi.org/10.1029/2003GL018526, 2003. 1360 Sun, L., Xue, L., Wang, T., Gao, J., Ding, A., Cooper, O. R., Lin, M., Xu, P., Wang, Z., Wang, X., Wen, 1361 L., Zhu, Y., Chen, T., Yang, L., Wang, Y., Chen, J., and Wang, W.: Significant increase of summertime 1362 ozone at Mount Tai in central eastern China, Atmos. Chem. Phys., 16, 10637-10650, 1363 https://doi.org/10.5194/acp-16-10637-2016, 2016. 1364 Sun, Z., Tan, J., Wang, F., Li, R., Zhang, X., Liao, J., Wang, Y., Huang, L., Zhang, K., Fu, J. S., and Li, 1365 L.: Regional background ozone estimation for China through data fusion of observation and simulation, 1366 Sci. Total Environ., 912, 169411, https://doi.org/10.1016/j.scitotenv.2023.169411, 2024. 1367 Sunwoo, Y., Carmichael, G. R., and Ueda, H.: Characteristics of background surface ozone in Japan,





- 1368 Atmos. Environ., 28, 25-37, https://doi.org/10.1016/1352-2310(94)90020-5, 1994.
- 1369 Thompson, T. M.: Background ozone: Challenges in science and policy, Congressional Research Service,
- 1370 Library of Congress, CRS Rep. R45482, 13 pp., 2019.
- 1371 Tsutsumi, Y., Zaizen, Y., and Makino, Y.: Tropospheric ozone measurement at the top of Mt. Fuji,
- 1372 Geophys. Res. Lett., 21, 1727-1730, https://doi.org/10.1029/94GL01107, 1994.
- 1373 U.S. EPA.: Air quality criteria for ozone and related photochemical oxidants (final report, 2006), U.S.
- Environmental Protection Agency, Washington, DC, EPA/600/R-05/004aF-cF, 2006.
- 1375 U.S. EPA.: Review of the national ambient air quality standards for ozone: Policy assessment of scientific
- 1376 and technical information, U.S. Environmental Protection Agency, Research Triangle Park, North
- 1377 Carolina, EPA-452/R-07-007, 2007.
- 1378 Valdes, P. J., Beerling, D. J., and Johnson, C. E.: The ice age methane budget, Geophys. Res. Lett., 32,
- 1379 L02704, https://doi.org/10.1029/2004GL021004, 2005.
- 1380 Vecchi, R. and Valli, G.: Ozone assessment in the southern part of the Alps, Atmos. Environ., 33, 97-109,
- 1381 https://doi.org/10.1016/S1352-2310(98)00133-2, 1998.
- Vingarzan, R.: A review of surface ozone background levels and trends, Atmos. Environ., 38, 3431-3442,
- 1383 https://doi.org/10.1016/j.atmosenv.2004.03.030, 2004.
- Volz, A. and Kley, D.: Evaluation of the Montsouris series of ozone measurements made in the nineteenth
- 1385 century, Nature, 332, 240-242, https://doi.org/10.1038/332240a0, 1988.
- 1386 Wang, F. T., Zhang, K., Xue, J., Huang, L., Wang, Y. J., Chen, H., Wang, S. Y., Fu, J. S., and Li, L.:
- 1387 Understanding regional background ozone by multiple methods: A case study in the Shandong region,
- 1388 China, 2018-2020, J. Geophys. Res.-Atmos., 127, e2022JD036809,
- 1389 https://doi.org/10.1029/2022JD036809, 2022.
- Wang, H., Jacob, D. J., Le Sager, P., Streets, D. G., Park, R. J., Gilliland, A. B., and van Donkelaar, A.:
- 1391 Surface ozone background in the United States: Canadian and Mexican pollution influences, Atmos.
- $1392 \qquad \quad Environ., 43, 1310\text{-}1319, \\ \text{https://doi.org/} 10.1016/j. \\ \text{atmosenv.} 2008.11.036, 2009a.$
- 1393 Wang, T., Wei, X. L., Ding, A. J., Poon, C. N., Lam, K. S., Li, Y. S., Chan, L. Y., and Anson, M.:
- 1394 Increasing surface ozone concentrations in the background atmosphere of southern China, 1994-2007,





1395 Atmos. Chem. Phys., 9, 6217-6227, https://doi.org/10.5194/acp-9-6217-2009, 2009b. 1396 Wang, Y., Zhang, Y., Hao, J., and Luo, M.: Seasonal and spatial variability of surface ozone over China: 1397 contributions from background and domestic pollution, Atmos. Chem. Phys., 11, 3511-3525, 1398 https://doi.org/10.5194/acp-11-3511-2011, 2011. 1399 Wang, Y., Zhao, Y., Liu, Y., Jiang, Y., Zheng, B., Xing, J., Liu, Y., Wang, S., and Nielsen, C. P.: Sustained 1400 emission reductions have restrained the ozone pollution over China, Nat. Geosci., 16, 967-974, 1401 https://doi.org/10.1038/s41561-023-01284-2, 2023. 1402 West, J. J. and Fiore, A. M.: Management of tropospheric ozone by reducing methane emissions, Environ. 1403 Sci. Technol., 39, 4685-4691, https://doi.org/10.1021/es048629f, 2005. 1404 Wilson, R. C., Fleming, Z. L., Monks, P. S., Clain, G., Henne, S., Konovalov, I. B., Szopa, S., and Menut, 1405 L.: Have primary emission reduction measures reduced ozone across Europe? An analysis of European 1406 rural background ozone trends 1996-2005, Atmos. Chem. Phys., 12, 437-454, 1407 https://doi.org/10.5194/acp-12-437-2012, 2012. 1408 Wu, L., Xue, L., and Wang, W.: Review on the observation-based methods for ozone air pollution 1409 research, Journal of Earth Environment, 8, 479-491, https://doi.org/10.7515/JEE201706001, 2017. 1410 Wu, S., Mickley, L. J., Jacob, D. J., Rind, D., and Streets, D. G.: Effects of 2000-2050 changes in climate 1411 and emissions on global tropospheric ozone and the policy-relevant background surface ozone in the 1412 United States, J. Geophys. Res.-Atmos., 113, 1-12, https://doi.org/10.1029/2007JD009639, 2008. 1413 Wuebbles, D. J. and Hayhoe, K.: Atmospheric methane and global change, Earth-Sci. Rev., 57, 177-210, 1414 https://doi.org/10.1016/S0012-8252(01)00062-9, 2002. 1415 Xie, M., Shu, L., Wang, T., Liu, Q., Gao, D., Li, S., Zhuang, B., Han, Y., Li, M., and Chen, P.: Natural 1416 emissions under future climate condition and their effects on surface ozone in the Yangtze River Delta 1417 region, China, Atmos. Environ., 150, 162-180, https://doi.org/10.1016/j.atmosenv.2016.11.053, 2017. 1418 Xie, W., Xing, Q., Xie, D., Wu, X., Hu, S., and Xu, W.: Pollution characteristics of ozone and its 1419 precursors in background region of Hainan Province, Environm. Sci., 43, 5407-5420, 1420 https://doi.org/10.13227/j.hjkx.202201027, 2022. 1421 Xu, J., Ma, J. Z., Zhang, X. L., Xu, X. B., Xu, X. F., Lin, W. L., Wang, Y., Meng, W., and Ma, Z. Q.:





1422 Measurements of ozone and its precursors in Beijing during summertime: Impact of urban plumes on 1423 ozone pollution in downwind rural areas, Atmos. Chem. Phys., 11, 12241-12252, 1424 https://doi.org/10.5194/acp-11-12241-2011, 2011. 1425 Xu, W., Lin, W., Xu, X., Tang, J., Huang, J., Wu, H., and Zhang, X.: Long-term trends of surface ozone 1426 and its influencing factors at the Mt Waliguan GAW station, China - Part 1: Overall trends and 1427 characteristics, Atmos. Chem. Phys., 16, 6191-6205, https://doi.org/10.5194/acp-16-6191-2016, 2016. 1428 Xu, W., Xu, X., Lin, M., Lin, W., Tarasick, D., Tang, J., Ma, J., and Zheng, X.: Long-term trends of 1429 surface ozone and its influencing factors at the Mt Waliguan GAW station, China - Part 2: The roles 1430 of anthropogenic emissions and climate variability, Atmos. Chem. Phys., 18, 773-798, 1431 https://doi.org/10.5194/acp-18-773-2018, 2018. 1432 Xu, X., Zhang, T., and Su, Y.: Temporal variations and trend of ground-level ozone based on long-term 1433 measurements in Windsor, Canada, Atmos. Chem. Phys., 19, 7335-7345, https://doi.org/10.5194/acp-1434 19-7335-2019, 2019. 1435 Xu, X., Lin, W., Xu, W., Jin, J., Wang, Y., Zhang, G., Zhang, X., Ma, Z., Dong, Y., Ma, Q., Yu, D., Li, Z., 1436 Wang, D., and Zhao, H.: Long-term changes of regional ozone in China: Implications for human health 1437 and ecosystem impacts, Elementa-Sci. Anthrop., 8, 13, https://doi.org/10.1525/elementa.409, 2020. 1438 Xue, L., Wang, T., Louie, P. K. K., Luk, C. W. Y., Blake, D. R., and Xu, Z.: Increasing external effects 1439 negate local efforts to control ozone air pollution: A case study of Hong Kong and implications for 1440 other Chinese cities, Environ. Sci. Technol., 48, 10769-10775, https://doi.org/10.1021/es503278g, 1441 2014. 1442 Xue, L. K., Wang, T., Zhang, J. M., Zhang, X. C., Deliger, Poon, C. N., Ding, A. J., Zhou, X. H., Wu, W. 1443 S., Tang, J., Zhang, Q. Z., and Wang, W. X.: Source of surface ozone and reactive nitrogen speciation 1444 at Mount Waliguan in western China: New insights from the 2006 summer study, J. Geophys. Res.-1445 Atmos., 116, 1-12, https://doi.org/10.1029/2010JD014735, 2011. 1446 Yamaji, K., Ohara, T., Uno, I., Tanimoto, H., Kurokawa, J., and Akimoto, H.: Analysis of the seasonal 1447 variation of ozone in the boundary layer in East Asia using the Community Multi-scale Air Quality 1448 model: What controls surface ozone levels over Japan?, Atmos. Environ., 40, 1856-1868,





- 1449 https://doi.org/10.1016/j.atmosenv.2005.10.067, 2006.
- 1450 Yan, Q., Wang, Y., Cheng, Y., and Li, J.: Summertime clean-background ozone concentrations derived
- from ozone precursor relationships are lower than previous estimates in the southeast United States,
- Environ. Sci. Technol., 55, 12852-12861, https://doi.org/10.1021/acs.est.1c03035, 2021.
- 1453 Ye, X., Zhang, L., Wang, X., Lu, X., Jiang, Z., Lu, N., Li, D., and Xu, J.: Spatial and temporal variations
- 1454 of surface background ozone in China analyzed with the grid-stretching capability of GEOS-Chem
- 1455 high performance, Sci. Total Environ., 914, 169909, https://doi.org/10.1016/j.scitotenv.2024.169909,
- 1456 2024.
- 1457 Yeo, M. J. and Kim, Y. P.: Long-term trends of surface ozone in Korea, J. Clean. Prod., 294, 125352,
- 1458 https://doi.org/10.1016/j.jclepro.2020.125352, 2021.
- 1459 Zeng, P., Lyu, X. P., Guo, H., Cheng, H. R., Jiang, F., Pan, W. Z., Wang, Z. W., Liang, S. W., and Hu, Y.
- Q.: Causes of ozone pollution in summer in Wuhan, central China, Environ. Pollut., 241, 852-861,
- 1461 https://doi.org/10.1016/j.envpol.2018.05.042, 2018.
- Zhang, L., Jacob, D. J., Downey, N. V., Wood, D. A., Blewitt, D., Carouge, C. C., van Donkelaar, A.,
- Jones, D. B. A., Murray, L. T., and Wang, Y.: Improved estimate of the policy-relevant background
- ozone in the United States using the GEOS-Chem global model with 1/2°×2/3° horizontal resolution
- over North America, Atmos. Environ., 45, 6769-6776, https://doi.org/10.1016/j.atmosenv.2011.07.054,
- 1466 2011.
- Zhang, Q. and Zhang, X.: Ozone spatial-temporal distribution and trend over China since 2013: Insight
- 1468 from satellite and surface observation, Environm. Sci., 40, 1132-1142,
- $1469 \qquad \qquad \text{https://doi.org/} 10.13227/j.hjkx.201808028, 2019. \\$
- 1470 Zhang, Y., Jin, J., Yan, P., Tang, J., Fang, S., Lin, W., Lou, M., Liang, M., Zhou, Q., Jing, J., Li, Y., Jia,
- 1471 X., and Lyu, S.: Long-term variations of major atmospheric compositions observed at the background
- 1472 stations in three key areas of China, Adv. Clim. Change Res., 11, 370-380,
- 1473 https://doi.org/10.1016/j.accre.2020.11.005, 2020.
- 1474 Zohdirad, H., Montazeri Namin, M., Ashrafi, K., Aksoyoglu, S., and Prévôt, A. S. H.: Temporal
- variations, regional contribution, and cluster analyses of ozone and NO_x in a middle eastern megacity

https://doi.org/10.5194/egusphere-2025-687 Preprint. Discussion started: 28 March 2025 © Author(s) 2025. CC BY 4.0 License.





1476 during summertime over 2017-2019, Environ. Sci. Pollut. Res., 29, 16233-16249,

1477 https://doi.org/10.1007/s11356-021-14923-1, 2022.